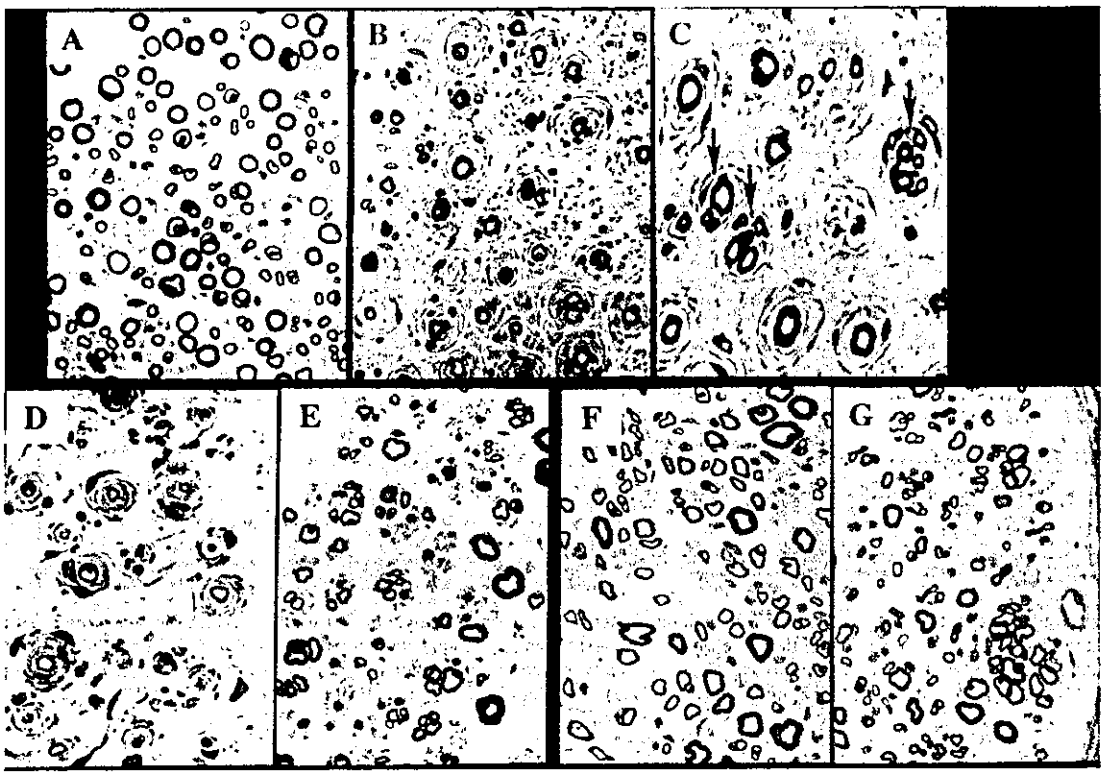

Fig. 3 (A) Transverse sections of the sural nerves from CMT patients. Myelinated fibre density was relatively well preserved but onion bulbs were rare in a 2-year-old patient with PMP22 duplication. (B) Myelinated fibre density was markedly decreased and onion bulb formation was prominent in a 43-year-old patient with PMP22 duplication. (C) Axonal sprouts were present at moderately density (arrows) in another patient with PMP22 duplication. (D and E) Onion bulb formation was prominent (D) in a patient with an MPZ mutation (Arg98His), while axonal sprouts were abundant (E) in another patient with an MPZ mutation (Thr124Met). Large myelinated fibres were significantly diminished in both of these patients. (F and G) Large myelinated fibre density was fairly well preserved in 16-year-old patient with a Cx32 mutation (Ser26Leu) (F), while they were markedly diminished and axonal sprouts were abundant (G) in a 61-year-old patient with a Cx32 mutation (Phe69Leu). Magnification: A, ×500; B, ×300; C, ×600; D–G, ×300.

≤38 m/s were seen concordantly among siblings in the 18 families in whom MCV was examined systemically (Table 4).

In MPZ mutations, probands with MCV ≤38 m/s in the median nerve (demyelinating subgroup) showed good concordance, with MCVs ≤38 m/s among siblings in the four families examined. Probands showing a median nerve MCV >38 m/s (axonal subgroup) exhibited good concordance, with MCV >38 m/s being noted among siblings in the four families (Table 4). The nature and position of amino acid substitutions in the MPZ protein were distinctly different among subgroups of patients with demyelinating and axonal phenotypes (Table 4), suggesting that demyelinating and axonal phenotypes in MCV are concordant in the siblings and are closely related to the nature and position of the amino acid substitution in MPZ.

In Cx32 mutations, the probands showed variable median nerve MCVs, including values more and less than 38 m/s. MCVs were discordant in terms of the 38 m/s cut-off value among siblings in the six families examined (Table 4). MCVs in these families were concordant among siblings in showing a range from 22.8 to 46.6 m/s. Thus, in most of the families, median nerve MCVs were discordant at the division point of 38 m/s but were concordant when the MCV range was set between 22.8 and 46.6 m/s (Table 4).

Muscle wasting, CMAPs and MCVs

Muscle weakness and atrophy were most pronounced in the distal portion of the leg and were noted to a lesser extent distally in the upper limbs; proximal muscles were only minimally involved. This distal and lower-limb-predominant motor involvement was common to all three main types of gene abnormality (Table 5). Table 6 shows the correlation between CMAPs and the strength of distal limb muscles in patients with PMP22 duplication, MPZ mutations and Cx32 mutations. The amplitude of CMAPs of median, ulnar and tibial nerves correlated significantly with corresponding distal muscle strengths ($r = 0.35$–0.69, $P < 0.05$–0.0005; Table 5).

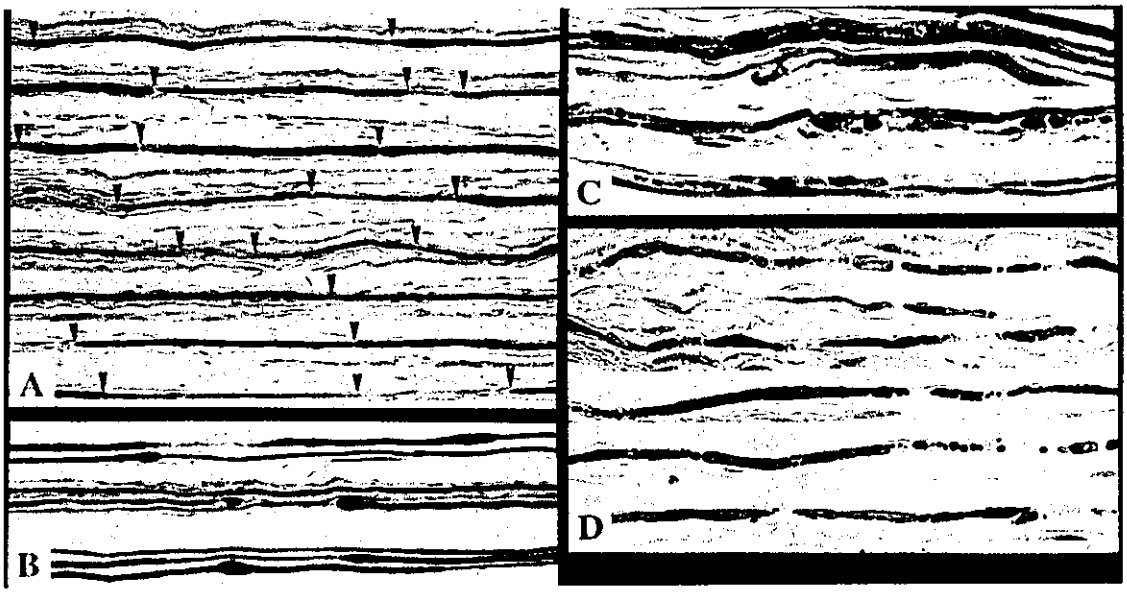

Fig. 4 (**A**) Teased fibres from the sural nerves of CMT patients. Extensive segmental demyelination was observed in a fibre from a patient with PMP22 duplication. Arrowheads indicate the node of Ranvier. (**B**) Globule or tomacula formation was abundant in another patient with PMP22 duplication. (**C** and **D**) Fibres with axonal degeneration were seen in an axonal subgroup of patients with an MPZ mutation (Thy124Met) (**C**) and in a patient with a Cx32 mutation (Phe69Leu) (**D**). Magnification: **A**, ×100; **B**, ×80; **C** and **D**, ×150.

In contrast, MCVs of median, ulnar and tibial nerves did not correlate with distal muscle strength in patients with PMP22 duplication, MPZ mutations or Cx32 mutations. These findings indicate that weakness in distal limb muscles was a consequence of reduced CMAP amplitude, not the slowing of MCV, in all groups.

Discussion

In CMT patients with PMP22 duplication, almost all patients showed predominantly demyelinating features in the nerve conduction study and pathological examination, with variable severity among individuals. MCVs were ⩽38 m/s, independently of age and disease duration. However, features of axonal loss, axonal sprouts and axonal changes in teased-fibre preparations as well as the decrease in CMAP amplitude were variably present irrespective of marked slowing of nerve conduction. These observations were in good agreement with previous reports (Kaku *et al.*, 1993*a*; Thomas *et al.*, 1997; Birouk *et al.*, 1997; Garcia *et al.*, 1998; Krajewski *et al.*, 2000; Dubourg *et al.*, 2001*a*). Since PMP22 duplication was shared among these patients, variability of demyelinating and axonal pathology between individual patients must be attributed to factors other than PMP22 duplication. Important factors demonstrated in this study were age and disease duration. CMAP reduction, axonal loss and onion bulb formation were more pronounced in advanced disease. Other factors could be the genetic background or environmental differences, as demonstrated in previous reports showing that the degree of reduction of nerve conduction was variable even in a family pedigree and in identical twins (Kaku *et al.*, 1993*a*, *b*; Garcia *et al.*, 1995, 1998; Birouk *et al.*, 1997). As reported so far, PMP22 duplication thus induces a mainly demyelinating phenotype, while features of axonal pathology are present concomitantly with advancing disease.

In cases with MPZ mutations, axonal and demyelinating phenotypes were clearly differentiated into two subgroups. Patients in the axonal subgroup rarely showed concomitant demyelinating phenotypes, and patients in the demyelinating subgroup rarely showed axonal features. These axonal or demyelinating phenotypes were also concordant among siblings in individual families. Furthermore, the nature and position of the MPZ gene mutation did not overlap between these two subgroups, indicating that axonal or demyelinating phenotypes are determined mainly by the nature and position of mutations of the MPZ gene. Apart from the MPZ gene mutation, the overall genetic background and environmental factors may have little effect on phenotypic variation in patients with the MPZ mutation. Age- and duration-dependent clinical and pathological changes could also be present, as was seen for PMP22 duplication, but we could not assess these issues because of relatively small numbers of patients in the subgroups.

Frequent association of neural deafness and pupillary abnormality in patients with the axonal phenotype of MPZ mutations was characteristic, confirming previous observations (Chapon *et al.*, 1999; De Jonghe *et al.*, 1999; Misu *et al.*, 2000). Prominent serum CK elevation was also more frequent

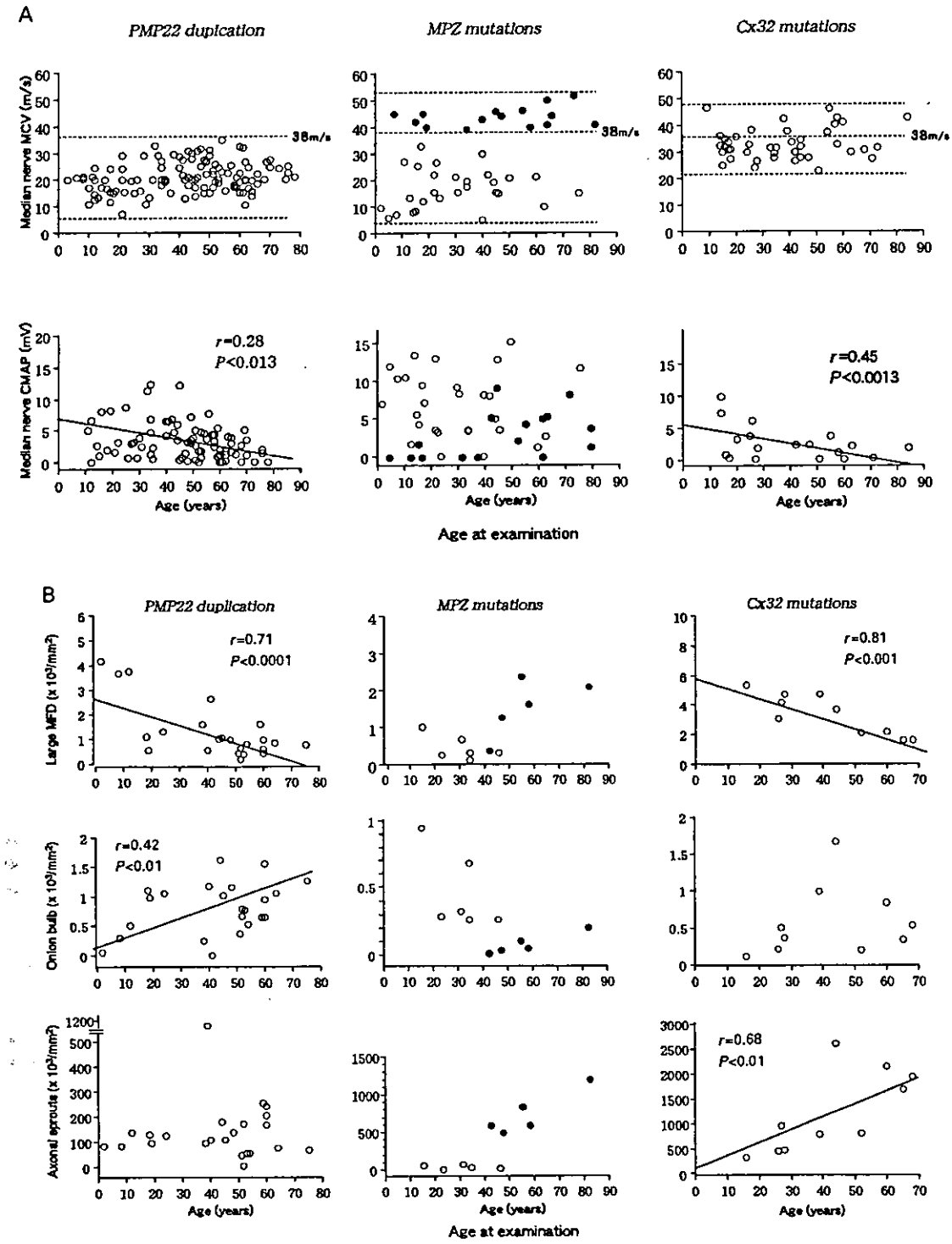

Fig. 5 Scattergrams of median nerve MCVs, CMAPs (A) and sural nerve pathology (B) in relation to age at examination in CMT patients. Closed circles and open circles in the panel labelled 'MPZ mutations' indicate patients with median nerve MCVs >38 m/s (corresponding to axonal phenotypes) and ≤38 m/s (corresponding to demyelinating phenotypes), respectively. In A, the dotted lines indicate the maximum and minimum values in each scattergram, and the 38 m/s level.

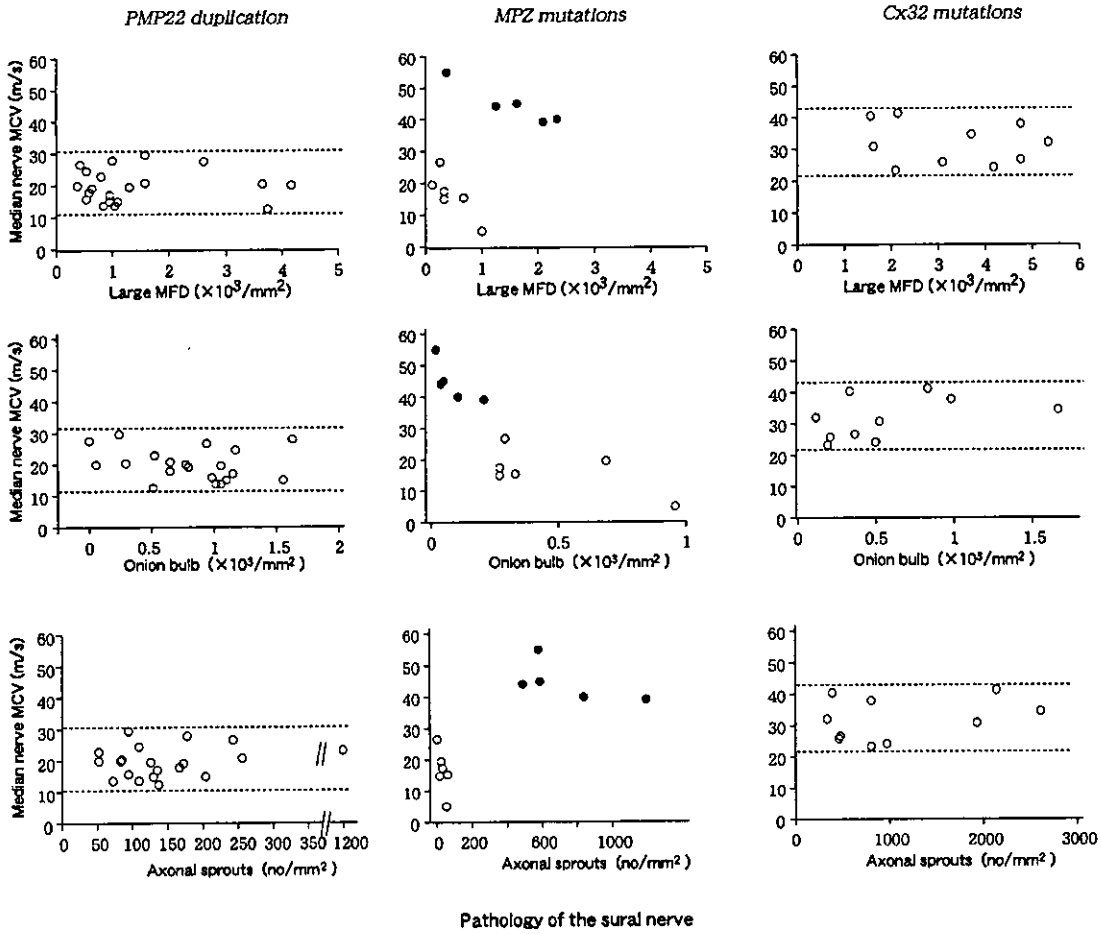

Fig. 6 Scattergrams of median nerve MCVs in relation to severity of sural nerve pathology [large myelinated fibre density (MFD), density of onion bulbs and axonal sprouts]. Closed circles and open circles in the panel labelled 'MPZ mutations' indicate patients with median nerve MCVs >38 m/s (corresponding to axonal phenotypes) and ≤38 m/s (corresponding to demyelinating phenotypes), respectively. Dotted lines indicate the maximum and minimum values in each scattergram.

in patients with MPZ mutation in the axonal subgroup. These associated symptoms were not restricted to specific MPZ mutations, but were widely present among patients with axonal phenotypes. These observations suggest that the mechanism that induces the axonal phenotype may also induce associated symptoms.

In Cx32 mutations, median nerve MCV was moderately slowed within a relatively restricted range of 22.8–46.6 m/s, confirming previous reports (Hahn *et al.*, 1990; Nicholson *et al.*, 1993, 1998; Dubourg *et al.*, 2001*a*, *b*). Pathologically, axonal features predominated but demyelinating features were present concomitantly, suggesting a mixture of axonal and demyelinating pathology. These MCVs and pathological phenotypes were independent of age and disease duration. However, other axonal markers, such as decreased CMAP amplitudes, axonal loss and axonal sprouts, were pronounced in patients with advanced disease. Cx32 mutations may induce both axonal and demyelinating features irrespective of the nature and position of the mutation in the Cx32 gene, with median MCVs showing a moderately decreased range.

Strikingly, median nerve MCVs were consistent independently of age, disease duration and pathological alterations in all three groups of genetic abnormality (Table 6). By consensus, the division point for axonal and demyelinating phenotypes of CMT has been considered to be 38 m/s for median nerve MCV (Dyck and Lambert, 1968; Buchthal and Behse, 1977; Harding and Thomas, 1980). Nerve conduction criteria for axonal and demyelinating phenotypes have been verified by observations in PMP22 duplication (Kaku *et al.*, 1993*a*, *b*; Nicholson and Nash, 1993; Nicholson *et al.*, 1998; Paraskevas *et al.*, 1998). In this study we confirmed the usefulness of this nerve conduction cut-off value in MPZ mutations. However, in Cx32 mutations, 38 m/s for median nerve MCV was not a useful division point. Median nerve

Table 4 *Gene mutations and median nerve MCV and concordance and discordance among siblings*

Gene mutations and median nerve MCV in the proband	Mutations	No. of families; MCV concordance and discordance among siblings in families examined systemically		
		Concordance to MCV ≤38 m/s	Concordance to MCV >38 m/s	Discordance to MCV ≤38 m/s and MCV >38 m/s
PMP22 duplication	Duplication of PMP22 gene	18 (2–5)	0	0
MPZ mutations				
MCV ≤38 m/s	Asp35Tyr, Ile62Phe, Ser63del, Tyr68Cys, Gly93Glu, Arg98Cys, Val146Phe	4 (2–4)	0	0
MCV >38 m/s	Asp75Val, His81Arg, Thr124Met Lys130Arg, Gly167Arg	0	4 (2–3)	0
Cx32 mutations	Ser26Leu, Thr55Ala, Gln57His, Val63Ile, Phe69Leu, Ser128stop, Val139Met, Arg142Gln, Arg142Trp, Pro172Arg, Val177Ala, Arg183His, Thr191Ala, Cys201Tyr, Ala282frameshift	1 (2)	0	6 (2–3)

Numbers in parentheses are number of patients in the family whose median nerve MCV was estimated.

Table 5 *Correlation between CMAP/MCV and muscle strength*

Mutations/nerves	*n*	*r*	*P*
PMP22 duplication			
Median			
CMAP vs distal MS	86	0.35	<0.0009
MCV vs distal MS	86	0.16	NS
Ulnar			
CMAP vs distal MS	63	0.44	<0.0005
MCV vs distal MS	63	0.05	NS
Posterior tibialis			
CMAP vs distal MS	79	0.36	<0.0014
MCV vs distal MS	79	0.15	NS
MPZ mutations			
Median			
CMAP vs distal MS	28	0.36	<0.05
MCV vs distal MS	28	0.05	NS
Ulnar			
CMAP vs distal MS	17	0.43	<0.05
MCV vs distal MS	17	0.14	NS
Posterior tibialis			
CMAP vs distal MS	17	0.47	<0.018
MCV vs distal MS	17	0.17	NS
Cx32 mutations			
Median			
CMAP vs distal MS	19	0.69	<0.0032
MCV vs distal MS	19	0.21	NS
Ulnar			
CMAP vs distal MS	19	0.68	<0.0079
MCV vs distal MS	19	0.30	NS
Posterior tibial			
CMAP vs distal MS	19	0.38	NS
MCV vs distal MS	19	0.16	NS

MS = muscle strength assessed as MRC score; distal MS = thenar and finger flexion muscles for the median nerves, interosseous muscles for the ulnar nerves, and triceps surae muscles and toe dorsiflexion muscles for the posterior tibial nerve. MS was assessed as MRC score for the examined muscles and averaged for the examined muscles for each individual.

MCV for Cx32 mutations ranged around 38 m/s but was restricted to a range between 22.8 and 46.6 m/s. The observation that median nerve MCVs are well maintained independently of age, disease duration and clinicopathological changes indicates that median nerve MCV is an excellent marker for genetically determined CMT phenotypes. In contrast, the amplitude of CMAPs, axonal loss (particularly for large axons), the density of axonal sprouts and onion bulb formation changed significantly with age and disease duration (Table 6). Distally accentuated muscular wasting was characteristic of all three genotypes and progressed with advancing age (Dyck *et al.*, 1989; Birouk *et al.*, 1997), showing good correlation with CMAP amplitude in the corresponding muscles. Disease duration, however, correlated less well with these features than did age at examination, suggesting that the disease process may begin early, at perinatal or embryonic stages, as suggested previously (Dyck *et al.*, 1989; Killian *et al.*, 1996; Garcia *et al.*, 1998). Disease duration, which represents the period after the disease process has crossed the clinical threshold, appears to correlate less well with the pathological changes and CMAPs than age at examination. Age-dependent decreases in CMAPs and increases in axonal pathology and clinical disability from neuropathic deficits were in good agreement with previous observations in CMT1 patients (Dyck *et al.*, 1989).

Taking all the results in this study together, we can identify two distinct clinicopathological phenotypic features, one that is independent of disease advancement and the other with changing phenotypic features according to disease advancement. The MCVs and the predominance of demyelinating or axonal phenotypes are included in the former category, and axonal features, such as CMAP amplitude, large-axon loss, axonal sprouts and distally accentuated muscle wasting, are included in the latter category. The present study shows that axonal features that change in relation to disease advance-

Table 6 *Demyelinating and axonal features of CMT patients*

Mutations	Disease advancement		Disease advancement-dependent				Correlation to muscle wasting
	Median nerve MCV	Predominant pathological phenotype	Decrease in CMAP	Axon loss	Axonal sprouts	Onion bulbs	
PMP22 duplication	≤38 m/s	Demyelinating	Yes	Yes	No	Yes	CMAP
MPZ mutations	≤38 m/s	Demyelinating	ND	ND	ND	ND	CMAP
	>38 m/s	Axonal	ND	ND	ND	ND	CMAP
Cx32 mutations	22.8 to 46.6 m/s	Axonal with mild demyelinating	Yes	Yes	Yes	No	CMAP

ND, not determined (sample size too small).

ment, particularly large-axon loss and decreased CMAP amplitude, constitute a major determinant of clinical manifestations such as muscle weakness and atrophy in all three common genotypic groups of CMT.

The molecular mechanisms that induce axonal involvement as disease advances, which have been demonstrated particularly in PMP22 duplication and Cx32 mutations, are poorly understood, and may differ among mutations. In the case of PMP22 duplication, axonal dysfunction could result from the primary process of demyelination, as suggested in previous studies (Dyck *et al.*, 1989; Garcia *et al.*, 1998; Sancho *et al.*, 1999; Scherer, 1999; Krajewski *et al.*, 2000). Local biochemical changes in axons, such as decreased neurofilament phosphorylation, increased neurofilament density and decreased axonal transport due to demyelinating Schwann cells, could accrue to produce axonal dysfunction and eventual axonal loss (de Waegh and Brady, 1990, de Waegh *et al.*, 1992; Watson *et al.*, 1994; Sahenk *et al.*, 1999). In Cx32 mutations, issues concerning mechanisms of progressive axonal involvement are further complicated, since an axonal phenotype is predominant but demyelinating features are concomitantly present to variable degrees in individual patients. Unknown mechanisms may induce axonal dysfunction and loss directly, while concomitant demyelinating features could also induce axon loss, as is suspected for PMP22 duplication. Studies using *in vivo* models with specific mutations of Cx32 and different genetic or environmental backgrounds are needed to provide better understanding of the molecular mechanisms.

The distally accentuated muscle wasting characteristic of CMT was strongly correlated with the reduction of the functioning large axonal population, as assessed by CMAPs, and was not correlated with slowing of nerve conduction. This finding was common to patients with PMP22 duplication, MPZ mutations and Cx32 mutations. Similar observations were reported in patients with PMP22 duplication (Krajewski *et al.*, 2000). In that report, muscle wasting and sensory impairment that was accentuated in the distal extremities correlated well with corresponding reductions in CMAPs and SNAPs, but not with slowing of motor and sensory nerve conduction. Our observations are in agreement with these reported observations in PMP22 duplication, while we have demonstrated further that clinical phenotypes of patients with MPZ and Cx32 mutations are also determined by reduction of the functioning large-axon population. Pathological study of autopsy cases of CMT with a hypertrophic form of extensive demyelination and an axonal form with massive axonal sprouting both demonstrated distally accentuated axon loss along peripheral nerve trunks that showed relatively well-preserved axons proximally (Smith *et al.*, 1980; Berciano *et al.*, 1986; Bird *et al.*, 1997). These pathological observations in CMT patients showing distally pronounced axon loss irrespective of the axonal or demyelinating phenotypes agree with the present study in showing distally accentuated muscle wasting in both axonal and demyelinating phenotypes.

In conclusion, our study demonstrates that three myelin-related protein gene abnormalities, PMP22 duplication, MPZ mutations and Cx32 mutations, resulted in a wide variety of demyelinating and axonal features. PMP22 duplication induced demyelinating changes; MPZ mutations induced distinctive subgroups with a demyelinating or axonal phenotype depending on the nature and position of the mutation; and Cx32 mutations induced predominant axonal and lesser demyelinating features essentially simultaneously. These genetically determined axonal and demyelinating phenotypes corresponded well with median nerve MCVs, which remained constant despite disease advancement. In contrast, clinical manifestations of muscle wasting correlated well with decreases in CMAPs and axonal loss, which became more pronounced as disease progressed.

Acknowledgements

This work was supported by a COE grant from the Ministry of Education, Science, Culture and Sports of Japan and grants from the Ministry of Health, Labour and Welfare of Japan. The following members of the Study Group for Hereditary Neuropathy in Japan were supported by the Ministry of

Health, Labour, and Welfare of Japan: Gen Sobue, Department of Neurology, Nagoya University Graduate School of Medicine; Ichiro Akiguchi, Department of Neurology, Kyoto University Graduate School of Medicine; Kiyoshi Hayasaka, Department of Pediatrics, Yamagata University School of Medicine; Masanori Nakagawa, Third Department of Internal Medicine, Kagoshima University Faculty of Medicine; Saburo Sakota, Department of Neurology, Osaka University Graduate School of Medicine; Kiichiro Matsumura, Department of Neurology, Teikyo University School of Medicine; Satoshi Onodera, Department of Neurology, Niigata University Graduate School of Medicine and Dental Sciences; Shu-ichi Ikeda, Department of Internal Medicine, Shinshu University School of Medicine; Takashi Yamamura, Department of Immunology, National Center of Neurology and Psychiatry; Yukio Ando, Department of Neurology, Kumamoto University School of Laboratory Medicine; Masayuki Baba, Department of Neurology, Hirosaki University School of Medicine; Masamitsu Nakazato, Third Department of Internal Medicine, Miyazaki Medical College; Hitoshi Yasuda, Third Department of Internal Medicine, Shiga University of Medical Sciences; Toyokazu Saito, Department of Neurology, Kitasato University School of Medicine; Kazuhiro Ikenaka, Department of Neural Information, National Institute for Physiology Laboratory; Jun-ichi Kira, Department of Neurology, Kyushu University Graduate School of Medicine; Keiji Wada, Department of Degenerative Neurological Diseases, National Center for Neurology and Psychiatry; Kenji Nakashima, Department of Neurological Sciences, Tottori University Faculty of Medicine; Kazuhiko Watabe, Department of Molecular Neuropathology, Tokyo Metropolitan Institute for Neurosciences; Ryuji Kaji, Division of Advanced Clinical Neuroscience, University of Tokushima School of Medicine; Nobuyuki Oka, Department of Internal Medicine, Hyogo College of Medicine; Eiko Ando, Department of Ophthalmology, Kumamoto National Hospital.

References

Baxter RV, Ben Othmane K, Rochelle JM, Stajich JE, Hulette C, Dew-Knight S, et al. Ganglioside-induced differentiation-associated protein-1 is mutant in Charcot–Marie–Tooth disease type 4A/8q21. Nature Genet 2002; 30: 21–2.

Berciano J, Combarros O, Figols J, Calleja J, Cabello A, Silos I, et al. Hereditary motor and sensory neuropathy type II. Clinicopathological study of a family. Brain 1986; 109: 897–914.

Bergoffen J, Scherer SS, Wang S, Scott MO, Bone LJ, Paul DL, et al. Connexin mutation in X-linked Charcot–Marie–Tooth disease. Science 1993; 262: 2039–42.

Bird TD, Kraft GH, Lipe HP, Kenney KL, Sumi SM. Clinical and pathological phenotype of the original family with Charcot–Marie–Tooth type 1B: a 20-year study. Ann Neurol 1997; 41: 463–9.

Birouk N, Gouider R, LeGuern E, Gugenheim M, Tardieu S, Maisonobe T, et al. Charcot–Marie–Tooth disease type 1A with 17p11.2 duplication. Clinical and electrophysiological phenotype study and factors influencing disease severity in 119 cases. Brain 1997; 120: 813–23.

Birouk N, LeGuern E, Maisonobe T, Rouger H, Gouider R, Tardieu S, et al. X-linked Charcot–Marie–Tooth disease with connexin32 mutations. Clinical and electrophysiologic study. Neurology 1998; 50: 1074–82.

Boerkoel CF, Takashima H, Garcia CA, Olney RK, Johnson J, Berry K, et al. Charcot–Marie–Tooth disease and related neuropathies: mutation distribution and genotype–phenotype correlation. Ann Neurol 2002; 51: 190–201.

Bolino A, Muglia M, Conforti FL, LeGuern E, Salih MA, Georgiou DM, et al. Charcot–Marie–Tooth type 4B is caused by mutations in the gene encoding myotubularin-related protein-2. Nature Genet 2000; 25: 17–9.

Bradley WG, Madrid R, Davis CJ. The peroneal muscular atrophy syndrome. J Neurol Sci 1977; 32: 123–36.

Buchthal F, Behse F. Peroneal muscular atrophy (PMA) and related disorders. I. Clinical manifestations as related to biopsy findings, nerve conduction and electromyography. Brain 1977; 100: 41–66.

Chapon F, Latour P, Diraison P, Schaeffer S, Vandenberghe A. Axonal phenotype of Charcot–Marie–Tooth disease associated with a mutation in the myelin protein zero gene. J Neurol Neurosurg Psychiatry 1999; 66: 779–82.

Cuesta A, Pedrola L, Sevilla T, Garcia-Planells J, Chumillas MJ, Mayordomo F, et al. The gene encoding ganglioside-induced differentiation-associated protein1 is mutated in axonal Charcot–Marie–Tooth type 4A disease. Nature Genet 2002; 30: 22–5.

De Jonghe P, Timmerman V, Ceuterick C, Nelis E, De Vriendt E, Lofgren A, et al. The Thr124Met mutation in the peripheral myelin protein zero (MPZ) gene is associated with a clinically distinct Charcot–Marie–Tooth phenotype. Brain 1999; 122: 281–90.

De Sandre-Giovannoli A, Chaouch M, Kozlov S, Vallat JM, Tazir M, Kassouri N, et al. Homozygous defects in LMNA, encoding lamin A/C nuclear-envelope proteins, cause autosomal recessive axonal neuropathy in human (Charcot–Marie–Tooth disease type 2) and mouse. Am J Hum Genet 2002; 70: 726–36.

de Waegh S, Brady ST. Altered slow axonal transport and regeneration in myelin-deficient mutant mouse: the trembler as an in vivo model for Schwann cell-axon interactions. J Neurosci 1990; 10: 1855–65.

de Waegh SM, Lee VM, Brady ST. Local modulation of neurofilament phosphorylation, axonal caliber, and slow axonal transport by myelinating Schwann cells. Cell 1992; 68: 451–63.

Dubourg O, Tardieu S, Birouk N, Gouider R, Leger JM, Maisonobe T, et al. Clinical, electrophysiological and molecular genetic characteristics of 93 patients with X-linked Charcot–Marie–Tooth disease. Brain 2001a; 124: 1958–67.

Dubourg O, Tardieu S, Birouk N, Gouider R, Leger JM, Maisonobe T, et al. The frequency of 17p11.2 duplication and Connexin 32 mutations in 282 Charcot–Marie–Tooth families in relation to the mode of inheritance and motor nerve conduction velocity. Neuromuscul Disord 2001b; 11: 458–63.

Dyck PJ, Lambert EH. Lower motor and primary sensory neuron diseases with peroneal muscular atrophy. I. Neurologic, genetic, and electrophysiologic findings in hereditary polyneuropathies. Arch Neurol 1968; 18: 603–18.

Dyck PJ, Kames JL, Lambert EH. Longitudinal study of neuropathic deficits and nerve conduction abnormalities in hereditary motor and sensory neuropathy type 1. Neurology 1989; 39: 1302–8.

Dyck PJ, Giannini C, Lais A. Pathologic alterations of nerves. In: Dyck PJ, Thomas PK, Griffin JW, Low PA, Poduslo JF, editors. Peripheral neuropathy. 3rd ed. Philadelphia: W.B. Saunders; 1993. p. 514–95.

Gabreels-Festen AA, Hoogendijk JE, Meijerink PH, Gabreels FJ, Bolhuis PA, van Beersum S, et al. Two divergent types of nerve pathology in patients with different P0 mutations in Charcot–Marie–Tooth disease. Neurology 1996; 47: 761–5.

Garcia CA, Malamut RE, England JD, Parry GS, Liu P, Lupski JR. Clinical variability in two pairs of identical twins with the Charcot–Marie–Tooth disease type 1A duplication. Neurology 1995; 45: 2090–3.

Garcia A, Combarros O, Calleja J, Berciano J. Charcot–Marie–Tooth disease type 1A with 17p duplication in infancy and early childhood: a longitudinal clinical and electrophysiologic study. Neurology 1998; 50: 1061–7.

Guilbot A, Williams A, Ravise N, Verny C, Brice A, Sherman DL, et al. A mutation in periaxin is responsible for CMT4F, an autosomal recessive form of Charcot–Marie–Tooth disease. Hum Mol Genet 2001; 10: 415–21.

Gutierrez A, England JD, Sumner AJ, Ferer S, Warner LE, Lupski JR, et al. Unusual electrophysiological findings in X-linked dominant Charcot–Marie–Tooth disease. Muscle Nerve 2000; 23: 182–8.

Hahn AF, Brown WF, Koopman WJ, Feasby TE. X-linked dominant hereditary motor and sensory neuropathy. Brain 1990; 113: 1511–25.

Hahn AF, Ainsworth PJ, Bolton CF, Bilbao JM, Vallat JM. Pathological findings in the x-linked form of Charcot–Marie–Tooth disease: a morphometric and ultrastructural analysis. Acta Neuropathol (Berl) 2001; 101: 129–39.

Harding AE. From the syndrome of Charcot, Marie and Tooth to disorders of peripheral myelin proteins. [Review]. Brain 1995; 118: 809–18.

Harding AE, Thomas PK. The clinical features of hereditary motor and sensory neuropathy types I and II. Brain 1980; 103: 259–80.

Hattori N, Ichimura M, Nagamatsu M, Li M, Yamamoto K, Kumazawa K, et al. Clinicopathological features of Churg–Strauss syndrome-associated neuropathy. Brain 1999; 122: 427–39.

Hayasaka K, Himoro M, Sato W, Takada G, Uyemura K, Shimizu N, et al. Charcot–Marie–Tooth neuropathy type 1B is associated with mutation of the myelin P0 gene. Nature Genet 1993; 5: 31–4.

Ikegami T, Ikeda H, Chance PF, Kiyosawa H, Yamamoto M, Sobue G, et al. Facilitated diagnosis of the CMT1A duplication in chromosome 17p11.2–12: analysis with a CMT1A-REP repeat probe and photostimulated luminescence imaging. Hum Mutat 1997; 9: 563–6.

Ionasescu V, Searby C, Ionasescu R. Point mutations of the connexin32 (GJB1) gene in X-linked dominant Charcot–Marie–Tooth neuropathy. Hum Mol Genet 1994; 3: 355–8.

Ionasescu VV, Searby C, Ionasescu R, Neuhaus IM, Werner R. Mutations of the noncoding region of the connexin32 gene in X-linked dominant Charcot–Marie–Tooth neuropathy. Neurology 1996; 47: 541–4.

Kaku DA, Parry GJ, Malamut R, Lupski JR, Garcia CA. Nerve conduction studies in Charcot–Marie–Tooth polyneuropathy associated with a segmental duplication of chromosome 17. Neurology 1993a; 43: 1806–8.

Kaku DA, Parry GJ, Malamut R, Lupski JR, Garcia CA. Uniform slowing of conduction velocities in Charcot–Marie–Tooth polyneuropathy type 1. Neurology 1993b; 43: 2664–7.

Kalaydjieva L, Gresham D, Gooding R, Heather L, Baas F, de Jonge R, et al. N-myc downstream-regulated gene 1 is mutated in hereditary motor and sensory neuropathy-Lom. Am J Hum Genet 2000; 67: 47–58.

Kamholz J, Menichella D, Jani A, Garbern J, Lewis RA, Krajewski KM, et al. Charcot–Marie–Tooth disease type 1: molecular pathogenesis to gene therapy. [Review]. Brain 2000; 123: 222–33.

Killian JM, Tiwari PS, Jacobson S, Jackson RD, Lupski JR. Longitudinal studies of the duplication form of Charcot–Marie–Tooth polyneuropathy. Muscle Nerve 1996; 19: 74–8.

Koike H, Mori K, Misu K, Hattori N, Ito H, Hirayama M, et al. Painful alcoholic polyneuropathy with predominant small-fiber loss and normal thiamine status. Neurology 2001; 56: 1727–32.

Kovach MJ, Lin JP, Boyadjiev S, Campbell K, Mazzeo L, Herman K, et al. A unique point mutation in the PMP22 gene is associated with Charcot–Marie–Tooth disease and deafness. Am J Hum Genet 1999; 64: 1580–93.

Krajewski KM, Lewis RA, Fuerst DR, Turansky C, Hinderer SR, Garbern J, et al. Neurological dysfunction and axonal degeneration in Charcot–Marie–Tooth disease type 1A. Brain 2000; 123: 1516–27.

Lupski JR, de Oca-Luna RM, Slaugenhaupt S, Pentao L, Guzzetta V, Trask BJ, et al. DNA duplication associated with Charcot–Marie–Tooth disease type 1A. Cell 1991; 66: 219–32.

Marrosu MG, Vaccargiu S, Marrosu G, Vannelli A, Cianchetti C, Muntoni F. Charcot–Marie–Tooth disease type 2 associated with mutation of the myelin protein zero gene. Neurology 1998; 50: 1397–401.

Matsunami N, Smith B, Ballard L, Lensch MW, Robertson M, Albertsen H, et al. Peripheral myelin protein-22 gene maps in the duplication in chromosome 17p11.2 associated with Charcot–Marie–Tooth 1A. Nature Genet 1992; 1: 176–9.

Mersiyanova IV, Perepelov AV, Polyakov AV, Sitnikov VF, Dadali EL, Oparin RB, et al. A new variant of Charcot–Marie–Tooth disease type 2 is probably the result of a mutation in the neurofilament-light gene. Am J Hum Genet 2000; 67: 37–46.

Misu K, Hattori N, Nagamatsu M, Ikeda S, Ando Y, Nakazato M, et al. Late-onset familial amyloid polyneuropathy type I (transthyretin Met30-associated familial amyloid polyneuropathy)

unrelated to endemic focus in Japan: clinicopathological and genetic features. Brain 1999; 122: 1951–62.

Misu K, Yoshihara T, Shikama Y, Awaki E, Yamamoto M, Hattori N, et al. An axonal form of Charcot–Marie–Tooth disease showing distinctive features in association with mutations in the peripheral myelin protein zero gene (Thr124Met or Asp75Val). J Neurol Neurosurg Psychiatry 2000; 69: 806–11.

Nagarajan R, Svaren J, Le N, Araki T, Watson M, Milbrandt J. EGR2 mutations in inherited neuropathies dominant-negatively inhibit myelin gene expression. Neuron 2001; 30: 355–68.

Nelis E, Van Broeckhoven C, De Jonghe P, Lofgren A, Vandenberghe A, Latour P, et al. Estimation of the mutation frequencies in Charcot–Marie–Tooth disease type 1 and hereditary neuropathy with liability to pressure palsies: a European collaborative study. Eur J Hum Genet 1996; 4: 25–33.

Nicholson G, Nash J. Intermediate nerve conduction velocities define X-linked Charcot–Marie–Tooth neuropathy families. Neurology 1993; 43: 2558–64.

Nicholson GA, Yeung L, Corbett A. Efficient neurophysiologic selection of X-linked Charcot–Marie–Tooth families: ten novel mutations. Neurology 1998; 51: 1412–6.

Paraskevas GP, Panousopoulou A, Karandreas N, Piperos P, Lygidakis C, Papageorgiou C. Correlation between denervation activity and compound muscle action potential amplitude in hereditary motor and sensory neuropathy I and II. Electromyogr Clin Neurophysiol 1998; 38: 343–7.

Patel PI, Roa BB, Welcher AA, Schoener-Scott R, Trask BJ, Pentao L, et al. The gene for the peripheral myelin protein PMP-22 is a candidate for Charcot–Marie–Tooth disease type 1A. Nature Genet 1992; 1: 159–65.

Raeymaekers P, Timmerman V, Nelis E, De Jonghe P, Hoogendijk JE, Baas F, et al. Duplication in chromosome 17p11.2 in Charcot–Marie–Tooth neuropathy type 1a (CMT 1a). The HMSN Collaborative Research Group. Neuromuscul Disord 1991; 1: 93–7.

Reilly MM. Classification of the hereditary motor and sensory neuropathies. [Review]. Curr Opin Neurol 2000; 13: 561–4.

Sahenk Z, Chen L, Mendell JR. Effects of PMP22 duplication and deletions on the axonal cytoskeleton. Ann Neurol 1999; 45: 16–24.

Sancho S, Magyar JP, Aguzzi A, Suterl U. Distal axonopathy in peripheral nerves of PMP22-mutant mice. Brain 1999; 122: 1563–77.

Sander S, Nicholson GA, Ouvrier RA, McLeod JG, Pollard JD. Charcot–Marie–Tooth disease: histopathological features of the peripheral myelin protein (PMP22) duplication (CMT1A) and connexin32 mutations (CMTX1). Muscle Nerve 1998; 21: 217–25.

Sander S, Ouvrier RA, Mcleod JG, Nicholson GA, Pollard JD. Clinical syndromes associated with tomacula or myelin swellings in sural nerve biopsies. J Neurol Neurosurg Psychiatry 2000; 68: 483–8.

Scherer S. Axonal pathology in demyelinating diseases [letter]. Ann Neurol 1999; 45: 6–7.

Scherer SS, Fischbeck KH. Is CMTX an axonopathy? [letter]. Neurology 1999; 52: 432–3.

Senderek J, Hermanns B, Bergmann C, Boroojerdi B, Bajbouj M, Hungs M, et al. X-linked dominant Charcot–Marie–Tooth neuropathy: clinical, electrophysiological, and morphological phenotype in four families with different connexin32 mutations (1). J Neurol Sci 1999; 167: 90–101.

Smith TW, Bhawan J, Keller RB, DeGirolami U. Charcot–Marie–Tooth disease associated with hypertrophic neuropathy: a neuropathologic study of two cases. J Neuropathol Exp Neurol 1980; 39: 420–40.

Sobue G, Hashizume Y, Mukai E, Hirayama M, Mitsuma T, Takahashi A, et al. X-Linked recessive bulbospinal neuronopathy: a clinicopathological study. Brain 1989; 112: 209–32.

Sobue G, Nakao N, Murakami K, Yasuda T, Sahashi K, Mitsuma T, et al. Type I familial amyloid polyneuropathy. A pathological study of the peripheral nervous system. Brain 1990; 113: 903–19.

Sobue G, Li M, Terao S, Aoki S, Ichimura M, Ieda T, et al. Axonal pathology in Japanese Guillain-Barré syndrome: a study of 15 autopsied cases. Neurology 1997; 48: 1694–700.

Tabaraud F, Lagrange E, Sindou P, Vandenberghe A, Levy N, Vallat JM. Demyelinating X-linked Charcot–Marie–Tooth disease: unusual electrophysiological findings. Muscle Nerve 1999; 22: 1442–7.

Thomas PK, Marques W Jr, Davis MB, Sweeney MG, King RH, Bradley JL, et al. The phenotypic manifestations of chromosome 17p11.2 duplication. Brain 1997; 120: 465–78.

Timmerman V, Nelis E, Van Hul W, Nieuwenhuijsen BW, Chen KL, Wang S, et al. The peripheral myelin protein gene PMP-22 is contained within the Charcot–Marie–Tooth disease type 1A duplication. Nature Genet 1992; 1: 171–5.

Vital A, Ferrer X, Lagueny A, Vandenberghe A, Latour P, Goizet C, et al. Histopathological features of X-linked Charcot–Marie–Tooth disease in 8 patients from 6 families with different connexin32 mutations. J Peripher Nerv Syst 2001; 6: 79–84.

Warner LE, Mancias P, Butler IJ, McDonald CM, Keppen L, Koob KG, et al. Mutations in the early growth response 2 (EGR2) gene are associated with hereditary myelinopathies. Nature Genet 1998; 18: 382–4.

Watson DF, Nachtman FN, Kuncl RW, Griffin JW. Altered neurofilament phosphorylation and beta tubulin isotypes in Charcot–Marie–Tooth disease type I. Neurology 1994; 44: 2383–7.

Yamamoto M, Yasuda T, Hayasaka K, Ohnishi A, Yoshikawa H, Yanagihara T, et al. Locations of crossover breakpoints within the CMT1A-REP repeat in Japanese patients with CMT1A and HNPP. Hum Genet 1997; 99: 151–4.

Yamamoto M, Keller MP, Yasuda T, Hayasaka K, Ohnishi A, Yoshikawa H, et al. Clustering of CMT1A duplication breakpoints in a 700 bp interval of the CMT1A-REP repeat. Hum Mutat 1998; 11: 109–13.

Yoshihara T, Yamamoto M, Doyu M, Mis KI, Hattori N, Hasegawa Y, et al. Mutations in the peripheral myelin protein zero and connexin32 genes detected by non-isotopic RNase cleavage assay and their phenotypes in Japanese patients with Charcot–Marie–Tooth disease. Hum Mutat (Online) 2000; 16: 177–8.

Yoshihara T, Kanda F, Yamamoto M, Ishihara H, Misu K, Hattori N, et al. A novel missense mutation in the early growth response 2 gene associated with late-onset Charcot–Marie–Tooth disease type 1. J Neurol Sci 2001; 184: 149–53.

Zhao C, Takita J, Tanaka Y, Setou M, Nakagawa T, Takeda S, et al. Charcot–Marie–Tooth disease type 2A caused by mutation in a microtubule motor KIF1Bbeta. Cell 2001; 105: 587–97.

Received May 2, 2002. Revised July 29, 2002.
Accepted July 29, 2002

Clinical and neuropathological correlates of Lewy body disease

Nozomi Hishikawa, Yoshio Hashizume, Mari Yoshida, Gen Sobue

[A1] Department of Neurology, Nagoya University Graduate School of Medicine, 65 Tsurumai-cho, Showa-ku, 466-8550, Nagoya, Japan
[A2] Institute for Medical Science of Aging, Aichi Medical University, Nagakute-cho, 480-1195, Aichi-gun, Japan

Abstract:

Abstract

We investigated distribution of neuronal and glial inclusions in 30 brains obtained at autopsy from patients with Lewy bodies (LBs) disease, which was clinically diagnosed as Parkinson's disease (PD), dementia with Lewy bodies (DLB), or pure autonomic failure (PAF). The cases were classified, according to the guidelines for the pathological diagnosis of DLB, into three types: the neocortical type, the limbic type, and the brain stem-predominant type. All postmortem brains had coil-like glial inclusions as well as LBs, and the distribution pattern and density of glial inclusions and LBs varied. The distribution of glial inclusions was strikingly similar to that of LBs. In the cerebral cortex in particular, the number of glial inclusions was fairly well correlated with the number of LBs, irrespective of the three pathological types. In the brain stem, distribution was similar between glial inclusions and LBs, and there was no distinct pathological difference among the three types. Glial inclusions and LBs were immunohistopathologically similar with respect to ubiquitin, f-synuclein, and Gallyas-Braak staining. The clinical features of the three types of LB disease were also similar; i.e., parkinsonism, some dementia, and/or autonomic failure. The inclusions in neurons and glial cells occurred in parallel with respect to tissue distribution and immunohistochemical features, suggesting that accumulation of neuronal and glial inclusions in the LB diseases have a common pathological feature. Our findings suggest that DLB, PD with and without dementia, and PAF share one clinicopathological entity.

Keywords:

Parkinson's disease, Dementia with Lewy body disease, Pure autonomic failure, Lewy body, α-synuclein

PAPER

Occipital hypoperfusion in Parkinson's disease without dementia: correlation to impaired cortical visual processing

Y Abe, T Kachi, T Kato, Y Arahata, T Yamada, Y Washimi, K Iwai, K Ito, N Yanagisawa, G Sobue

J Neurol Neurosurg Psychiatry 2003;**74**:419–422

See end of article for authors' affiliations

Correspondence to: Dr Y Abe, Department of Neurology, Chubu National Hospital, Obu, Aichi 474–8511, Japan; yujiabe@chubu-nh.go.jp

Received 5 August 2002
Accepted in revised form 22 October 2002

Objective: The purpose of this study was to analyse changes in regional cerebral blood flow (rCBF) in Parkinson's disease (PD) without dementia.
Methods: Twenty eight non-demented patients with PD and 17 age matched normal subjects underwent single photon emission computed tomography with N-isopropyl-p-[^{123}I]iodoamphetamine to measure rCBF. The statistical parametric mapping 96 programme was used for statistical analysis.
Results: The PD patients showed significantly reduced rCBF in the bilateral occipital and posterior parietal cortices ($p<0.01$, corrected for multiple comparison $p<0.05$), when compared with the control subjects. There was a strong positive correlation between the score of Raven's coloured progressive matrices (RCPM) and the rCBF in the right visual association area ($p<0.01$, corrected for multiple comparison $p<0.05$) among the PD patients.
Conclusions: This study showed occipital and posterior parietal hypoperfusion in PD patients without dementia. Furthermore, it was demonstrated that occipital hypoperfusion is likely to underlie impairment of visual cognition according to the RCPM test, which is not related to motor impairment.

It has been reported in previous studies that patients with Parkinson's disease (PD), even those without dementia, showed changes in regional cerebral blood flow (rCBF).[1–8] However, the findings of these investigations have been inconsistent. Frontal[1 2] parietal,[3], temporal,[4] or global[1 3] cortical hypoperfusion, or unchanged blood flow[4–8] have been reported. This inconsistency is considered to be attributable, not only to the heterogeneity among PD patients, but also to the lack of standardisation of image-analysing methods. In most previous studies, visually placed region of interest (ROI) analysis methods were used to evaluate the alterations of rCBF. This approach is limited in that the manual placement of ROI gives rise to the observer biases and large areas of the brain are left unexplored.

Statistical parametric mapping (SPM), developed by Frinston *et al*, is a voxel based statistical technique that is used to examine regional changes in imaging data.[9 10] This is entirely automated and objective, and can completely overcome the disadvantage of earlier ROI analysis methods. Recently, the SPM programme has been widely used to examine regional dysfunction of the brain in various neurological diseases.[11–13]

The purpose of this study was to analyse the rCBF in PD patients without dementia on a voxel by voxel basis using single photon emission computed tomography (SPECT) with N-isopropyl-p-[^{123}I]iodoamphetamine (^{123}I-IMP) and the SPM programme. We compared the rCBF in PD patients to that in age matched normal subjects. In addition, we investigated the relation between the rCBF and clinical features in PD patients.

Table 1 Clinical features of subjects

	Normal controls (n=17)	Patients with Parkinson's disease (n=28)
Age (y)*	69.6(10.2)	67.3 (7.3)
Sex (F/M)	9/8	17/11
Duration of illness (y)*		8.6 (4.6)
UPDRS motor score*		35.2 (12.9)

*Mean (SD).

METHODS

Subjects

Twenty eight PD patients without dementia and 17 age matched normal control subjects were included in this study (table 1). The 28 PD patients were diagnosed with the United Kingdom Parkinson's Disease Society Brain Bank criteria for clinical diagnosis of idiopathic PD,[14] and the extrapyramidal symptoms were scored according to the motor examination score of the Unified Parkinson's Disease Rating Scale (UPDRS).[15] Patients who had visual hallucination were excluded. No abnormal intensity or obvious cortical atrophy was seen on magnetic resonance imaging of the brain of any patient. None of the patients had any other illnesses or were taking any medication, except for antiparkinsonian drugs. All 28 patients had been taking levodopa treatment at the time of SPECT scanning. In addition, dopamine receptor agonists had been used in 12 patients, six patients had been treated with low dose anticholinergic agents, droxydopa had been given to two patients, and three patients had been taking amantadine hydrochloride.

None of the 17 normal control subjects had a history of any neurological or psychiatric disorders, and the neurological examination of each control subject was normal.

All of the PD and control subjects were assessed using the mini-mental state examination (MMSE),[16] and 25 PD patients and 14 control subjects also took the Raven's coloured progressive matrices (RCPM).[17] For both SPECT scanning and cognitive test, all patients were examined after overnight withdrawal of medication.

Informed consent was obtained from every subject before the study. Permission to perform this study was obtained from the ethical committee of Chubu National Hospital.

Abbreviations: PD, Parkinson's disease; rCBF, regional cerebral blood flow; RCPM, Raven's coloured progressive matrices; MMSE, mini-mental state examination; ROI, region of interest; SPM, statistical parametric mapping

Image acquisition

^{123}I-IMP (Nihon Mediphysics, Hyogo, Japan), 222 MBq (6 mCi), was injected into an antecubital vein while the subjects laid in a supine position with eyes closed in a quiet room. A single blood sample was obtained from the brachial artery between 9 and 10 minutes after the ^{123}I-IMP administration. SPECT scanning was carried out between 15 and 45 minutes after injection using a two head rotating GCA 7200DI gammacamera (Toshiba, Tokyo, Japan) fitted with low energy, high resolution collimators. The data were acquired in a 128×128 matrix through a 180° rotation at an angle interval of 4°. The projection data were prefiltered through a Butterworth filter, and then reconstructed using a Ramp backprojection filter. Chang's attenuation correction[18] and scattering correction using the triple energy window method[19] were applied to the reconstructed images. The in-plane spatial resolution was 11.1 mm in full width at half maximum (FWHM). The final image slices were set up parallel to the orbitomeatal line and were obtained at an interval of 3.44 mm through the entire brain. The rCBF images were quantitated according to the IMP-ARG method.[20] This method is based on the two compartment model for tracer kinetics, and uses a standard arterial input calibrated by the radioactivity of a single arterial whole blood sample, a standard lipophilic fraction of ^{123}I-IMP in whole blood and fixed distribution volume of ^{123}I-IMP. All images were transferred to a Sun workstation (Sun Microsystems, Mountain View, CA, USA) for further analysis.

Data analysis

The data were analysed using the statistical parametric mapping 96 (SPM96; Wellcome Department of Cognitive Neurology, Institute of Neurology, London, UK)[9 10] implemented in MATLAB (Math Works, Sherborn, MA, USA). Each image was transformed into the standard anatomical space with the programme provided by the Montreal Neurological Institute.[21] All of the images resulting from the normalisation procedure were visually acceptable. The global CBF of PD patients was 49.5 (9.9) ml/100g/min (mean (SD)), and that of normal controls was 52.4 (13.1) ml/100g/min. There was no significant difference of the mean global CBF in the two groups, but the apparent interindividual variation of the global CBF was seen in each group. Therefore, in the following analyses, proportional scaling was applied to adjust the mean whole brain activity to 50 ml/100 g/min to avoid interindividual variation in global CBF. The grey matter threshold was 0.8.

For comparison between the PD group and the control group, the normalised images of the non-demented patients with PD and those of the normal subjects were compared by a voxel by voxel *t* statistics. The resulting statistical parametric maps of *t* statistics, SPM{t}, were transformed to maps of the unit normal distribution, SPM{z}. The statistical significance was chosen at a level of $z>2.33$ (equivalent to an uncorrected $p<0.01$). To correct for multiple comparisons, the significance of the difference between each detected brain region was estimated using distributional approximations from theory of Gaussian field, in terms of spatial extent and peak height. A corrected p value of 0.05 was used as the final threshold for significance.

Next, we compared the images of the PD patients to examine whether there were any voxels in which the rCBF was significantly correlated with various clinical characteristics including the duration of illness, the UPDRS motor score, the MMSE score, and the RCPM score. Each value of the clinical characteristics was used as a covariate of interest, and both the values of the global rCBF and age were used as confounding covariates. The statistical significance was chosen at a level of $z>2.33$ (equivalent to an uncorrected $p<0.01$). A corrected p value of 0.05 was chosen in multiple comparisons.

Table 2 Brain regions in which the rCBF of the PD group was significantly lower than that of the normal control group (SPM analysis)

Cerebral region	Brodmann's area	x	y	z	Z
L middle occipital gyrus	18, 19, 39	-34	-78	8	4.63
R middle occipital gyrus	18, 19, 39	28	-84	14	4.28
L angular gyrus	39	-46	-54	34	3.43
R angular gyrus	39	44	-56	38	3.98
L cuneus	18	-26	-86	0	3.37
R cuneus	18	8	-88	14	2.57
L calcarine sulcus	17	-18	-94	-8	3.69
L precuneus	7	-10	-70	42	3.37
L lingual gyrus	18	-18	-84	-16	3.36
L superior occipital gyrus	19	-32	-84	30	3.34
L superior parietal lobule	7	-12	-72	52	3.23

x, y, z=coodinates of the peak in the standard anatomical space; Z=Z score of maximal peak; L=left; R=right. $p<0.01$, corrected for multiple comparisons.

RESULTS

Clinical manifestations

The total UPDRS motor examination score ranged from 3 to 56, and the mean (SD) score was 34.8 (13.2). The mean MMSE score of the 28 PD patients was 28.1 (2.1) (range, 25 to 30), and that of the 17 control subjects was 28.5 (2.0) (range, 25 to 30). The MMSE score of the PD group did not differ significantly from that of the control group. The mean RCPM score was 24.4 (5.2) (range, 16 to 33) for the 25 PD patients, and was 28.2 (3.5) (range, 25 to 34) for the 10 control subjects. The RCPM score of the PD group was significantly lower than that of the control group ($p<0.05$).

There was no correlation between the age, the duration of illness, the UPDRS motor examination score, the MMSE score, and the RCPM score in the PD group.

Comparison of the rCBF between the PD and normal control groups

Twenty eight PD patients without dementia and 17 control subjects underwent SPECT scanning, and the images of the PD and control groups were compared. According to SPM analysis, the rCBF in the bilateral occipital cortices and the bilateral posterior parietal cortices in the PD group were significantly lower than those in the respective area in the control group ($p<0.01$, corrected $p<0.05$) (table 2, fig 1).

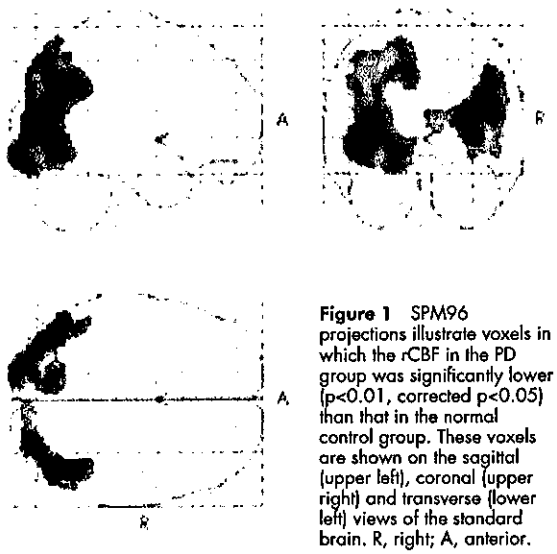

Figure 1 SPM96 projections illustrate voxels in which the rCBF in the PD group was significantly lower ($p<0.01$, corrected $p<0.05$) than that in the normal control group. These voxels are shown on the sagittal (upper left), coronal (upper right) and transverse (lower left) views of the standard brain. R, right; A, anterior.

Table 3 Brain regions in which there was a positive correlation between the RCPM score and the rCBF among 25 PD patients (SPM analysis)

Cerebral region	Brodmann's area	x	y	z	Z
R angular gyrus	39	46	-66	24	4.36
R middle occipital gyrus	19	40	-70	18	4.34
R inferior parietal lobule	40	42	-50	46	3.09

x, y, z=coodinates of the peak in the standard anatomical space; Z=Z score of maximal peak; R=right. p<0.01, corrected for multiple comparisons.

There was no brain region in which the rCBF was significantly higher in the PD group than in the control group.

Correlation between clinical characteristics and rCBF in the PD patients without dementia

There was a positive correlation between the RCPM score and the rCBF in the right dorsolateral occipital and the right posterior parietal cortices ($p<0.01$, corrected $p<0.05$) among 25 PD patients (table 3, fig 2). In most of these regions, the rCBF was reduced significantly in the PD group compared with the normal control group. There was no correlation between the duration of illness, the UPDRS motor examination score, or the MMSE score and the value of rCBF for any brain region.

DISCUSSION

This study showed that the rCBF in the non-demented PD patients was significantly lower than that in the age matched normal subjects in the bilateral occipital and posterior parietal cortices. It is well known that patients with PD, even those who do not have dementia, often develop various kinds of cognitive abnormalities that are closely related to visual dysfunction. Loss of luminance and colour contrast sensitivity and the impairment in preattentive cortical visual processing have been reported.[22-24] Furthermore, neuropsychological studies have revealed that PD patients have visuospatial deficit.[25 26] It seems appropriate to conclude that occipital dysfunction is a common feature of PD patients without dementia.

Actually, in our study, the mean RCPM score in the PD group was significantly lower than that in the normal control group, although the MMSE score of the PD group and that of the control group did not differ. RCPM is used for evaluation of visual perception, especially visuospatial attention, as the person taking the test must visually analyse form, colour, and linear slope.[27] Moreover, RCPM is one of the most appropriate batteries to test visual perceptual function purely, because it requires very little motor response. Therefore, in PD patients, the RCPM score is not likely to be affected by the poor motor ability. In fact, the RCPM score did not correlate to the UPDRS motor score in our PD patients. The impairment in RCPM test is clearly distinct from dementia, and is not considered to be secondary to the motor dysfunction.

In this study, we found that there was a strong positive correlation between the RCPM score and the rCBF in the right dorsolateral occipital area, corresponding to the visual association cortex, and the right posterior parietal area among non-demented PD patients. In these areas, there was no correlation between the UPDRS motor score and the rCBF, therefore, it may be reasonable to suppose that the reduction of rCBF in the visual association area purely reflects the impairment in cortical visual processing. Although some previous studies demonstrated occipital hypoperfusion and glucose hypometabolism,[9 28-31] there has been no previous study showing that the correlation between occipital hypometabolism or hypoperfusion and clinical abnormality related with visual

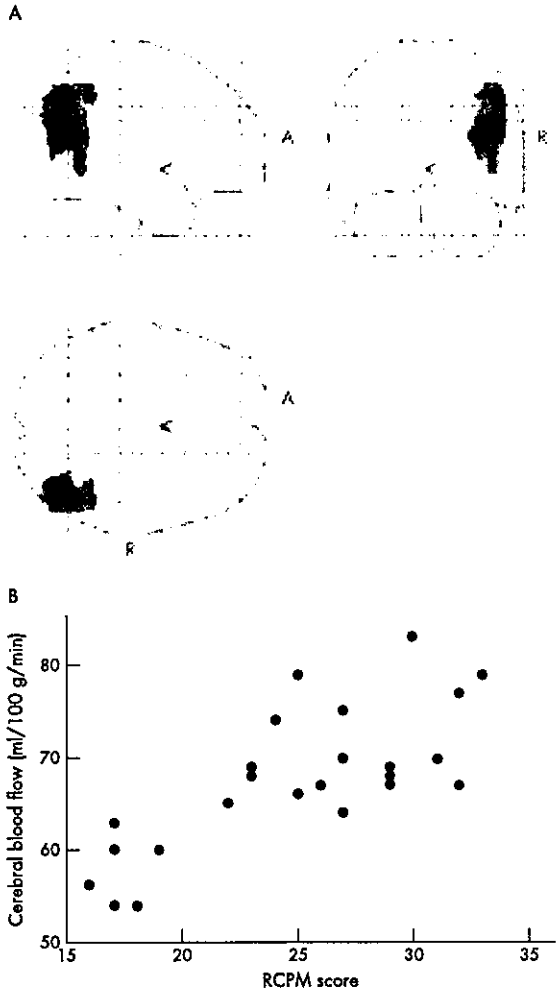

Figure 2 (A) SPM96 projections illustrate voxels in which there is a positive correlation ($p<0.01$, corrected $p<0.05$) between the RCPM score and the rCBF among 25 PD patients. R, right; A, anterior. (B) Scatter plot between the RCPM score and the rCBF at the voxel in the right middle occipital gyrus where there is a positive correlation ($p<0.005$, $r=0.73$, Spearman's correlation coefficient by ranks) between the RCPM score and the rCBF. *The mean whole brain activity was adjusted to 50 ml/100 g/min.

dysfunction was directly proved. This is the first study to demonstrate this correlation. The reason why the correlation was seen only in the right hemisphere is not clear, but this is possibly associated with the dominance of the right hemisphere in visuospatial attention.[32 33]

The underlying mechanism of the reduction of rCBF in the occipital lobe of PD patients remains unknown. In the previous report, a reduction of amplitude in the pattern electroretinogram[34] was demonstrated in PD patients. This abnormality has been considered to be attributable to diminished dopaminergic neurons in the retina, and this retinal dysfunction may be responsible for the occipital hypoperfusion. Furthermore, PD patients may have primary pathological findings in the cortices. However, morphological studies have not disclosed primary abnormalities, such as neuronal loss, gliosis, and appearance of Lewy bodies, in these brain regions in non-demented PD patients.[35 36] Another explanation, which seems much more plausible, is a functional deficit of the cortex that results from damage to the

subcortical structure. There is considerable evidence supporting the presence of a corticostriatal projection which arises from the entire cortical region and projects to the striatum.[37 38] The compact zone of the substantia nigra also gives off efferents to the striatum, and is widely believed to modify the activity of the cortical output to the striatum.[37 38] Therefore, the loss of nigrostriatal neurons may impair the association between the cortical region and the striatum, and consequently may reduce cortical activity. The research group of Denny-Brown and Yanagisawa reported the intimate functional connection between the visual association areas and the striatum.[39 40] They demonstrated in monkeys that extensive destruction of the posterior part of the putamen was followed by a remarkable loss of visual attention and inhibition of grasp and traction response, and that these signs also resulted from destruction of the visual association cortex and the posterior parietal cortex. The physical connection of the visual association cortex and the posterior parietal cortex with the posterior part of the putamen was also described by Kemp and Powell.[41]

It is difficult to detect the correlation between RCPM score and the rCBF in the dorsolateral visual association areas, if conventional ROI analysis methods had been used. Because the dorsolateral visual association area is located around the parieto-occipital junction, most investigators avoid setting of ROIs in this area. On the other hand, using the SPM program, whole brain lesions can be explored by a voxel based statistical technique. It has become possible using the SPM program to detect that occipital hypoperfusion is related to the visual dysfunction according to the RCPM test.

In conclusion, we confirmed that occipital hypoperfusion is a common feature of PD patients without dementia. It was demonstrated that occipital hypoperfusion is likely to reflect the visual impairment examined with the RCPM test that is not related to the motor impairment.

Authors' affiliations
Y Abe, K Iwai, G Sobue, Department of Neurology, Nagoya University School of Medicine, Nagoya, Japan
Y Abe, T Kachi, Y Arahata, T Yamada, Y Washimi, K Iwai, Department of Neurology, Chubu National Hospital, Aichi, Japan
T Kato, K Ito, Department of Biofunctional Research, National Institute for Longevity Sciences, Aichi, Japan
N Yanagisawa, Department of Neurology, Kanto Rosai Hospital, Kanagawa, Japan

Funding: this research was partly supported by a Health Sciences Research Grant for Comprehensive Research on Aging and Health and a Health Sciences Research Grant for Research on Brain Science from the Ministry of Health, Labour and Welfare of Japan.

Competing interests: none declared.

REFERENCES

1 **Wolfson LI,** Leenders KL, Brown LL, *et al.* Alterations of regional cerebral blood flow and oxygen metabolism in Parkinson's disease. *Neurology* 1985;**35**:1399–405.
2 **Defebvre L,** Lecouffe P, Destee A, *et al.* Tomographic measurements of regional cerebral blood flow in progressive supranuclear palsy and Parkinson's disease. *Acta Neurol Scand* 1995;**92**:235–41.
3 **Tachibana H,** Kawabata K, Tomino Y, *et al.* Brain perfusion imaging in Parkinson's disease and Alzheimer's disease demonstrated by three-dimensional surface display with 123I-iodoamphetamine. *Dementia* 1993;**4**:334–41.
4 **Jagust WJ,** Reed BR, Martin EM, *et al.* Cognitive function and regional cerebral blood flow in Parkinson's disease. *Brain* 1992;**115**:521–37.
5 **Imon Y,** Matsuda H, Ogawa M, *et al.* SPECT image analysis using statistical parametric mapping in patients with Parkinson's disease. *J Nucl Med* 1999;**40**:1583–9.
6 **Perlmutter JS,** Raichle ME. Regional blood flow in hemiparkinsonism. *Neurology* 1985;**35**:1127–34.
7 **Spampinato U,** Habert MO, Mas JL, *et al.* (^{99m}Tc)-HM-PAO SPECT and cognitive impairment in Parkinson's disease: a comparison with dementia of the Alzheimer type. *J Neurol Neurosurg Psychiatry* 1991;**54**:787–92.
8 **Wang SJ,** Liu RS, Liu HC, *et al.* Technetium-99m hexamethylpropylene amine oxime single photon emission tomography of the brain in early Parkinson's disease: correlation with dementia and lateralization. *Eur J Nucl Med* 1993;**20**:339–44.
9 **Friston KJ,** Ashburner J, Frith CD, *et al.* Spatial registration and normalization of images. *Hum Brain Mapp* 1995;**3**:165–89.
10 **Friston KJ,** Holmes AP, Worsley KJ, *et al.* Statistical parametric maps in functional imaging: a general linear approach. *Hum Brain Mapp* 1995;**2**:189–210.
11 **Roelcke U,** Kappos L, Lechner-Scott J, *et al.* Reduced glucose metabolism in the frontal cortex and basal ganglia of multiple sclerosis patients with fatigue: a ^{18}F-fluorodeoxyglucose positron emission tomography study. *Neurology* 1997;**48**:1566–71.
12 **Desgranges B,** Baron JC, de la Sayette V, *et al.* The neural substrates of memory systems impairment in Alzheimer's disease. A PET study of resting brain glucose utilization. *Brain* 1998;**121**:611–31.
13 **Van Bogaert P,** David P, Gillain CA, *et al.* Perisylvian dysgenesis. Clinical, EEG, MRI and glucose metabolism features in 10 patients. *Brain* 1998;**121**:2229–38.
14 **Hughes AJ,** Daniel SE, Kilford L, *et al.* Accuracy of clinical diagnosis of idiopathic Parkinson's disease: a clinico-pathological study of 100 cases. *J Neurol Neurosurg Psychiatry* 1992;**55**:181–4.
15 **Fahn S,** Elton RL, Members of the UPDRS Development Committee. Unified Parkinson's disease rating scale. In: Fahn S, Marsden CD, Calne DB, *et al*, eds. *Recent development in Parkinson's disease.* Florham Park NJ: MacMillan Healthcare Information, 1987:153–63, 293–304.
16 **Folstein MF,** Folstein SE, McHugh PR. "Mini-mental state". A practical method for grading the cognitive state of patients for the clinician. *J Psychiatr Res* 1975;**12**:189–98.
17 **Raven J.** *Guide to using the coloured progressive matrices.* London: Lewis, 1965.
18 **Chang LT.** A method for attenuation correction in radionuclide computed tomography. *IEEE Trans Nucl Sci* 1978;**25**:638–43.
19 **Ogawa K.** A practical method for position-dependent compton-scatter correction in single photon emission CT. *IEEE Trans Med Imaging* 1991;**10**:408–12.
20 **Iida H,** Itoh H, Nakazawa M, *et al.* Quantitative mapping of regional cerebral blood flow using iodine-123-IMP and SPECT. *J Nucl Med* 1994;**35**:2019–30.
21 **Evans AC,** Collins DL, Milner B. An MRI-based stereotactic atlas from 250 young normal subjects. *Soc Neurosci Abstr* 1992;**18**:408.
22 **Bodis-Wollner I,** Marx MS, Mitra S, *et al.* Visual dysfunction in Parkinson's disease. Loss in spatiotemporal contrast sensitivity. *Brain* 1987;**110**:1675–98.
23 **Haug BA,** Kolle RU, Trenkwalder C, *et al.* Predominant affection of the blue cone pathway in Parkinson's disease. *Brain* 1995;**118**:771–8.
24 **Lieb K,** Brucker S, Bach M, *et al.* Impairment in preattentive visual processing in patients with Parkinson's disease. *Brain* 1999;**122**:303–13.
25 **Pirozzolo FJ,** Hansch EC, Mortimer JA, *et al.* Dementia in Parkinson disease: a neuropsychological analysis. *Brain Cogn* 1982;**1**:71–83.
26 **Boller F,** Passafiume D, Keefe NC, *et al.* Visuospatial impairment in Parkinson's disease. Role of perceptual and motor factors. *Arch Neurol* 1984;**41**:485–90.
27 **Tanaka F,** Kachi T, Yamada T, *et al.* Auditory and visual event-related potentials and flash visual evoked potentials in Alzheimer's disease: correlations with Mini-Mental State Examination and Raven's coloured progressive matrices. *J Neurol Sci* 1998;**156**:83–8.
28 **Peppard RF,** Martin WR, Carr GD, *et al.* Cerebral glucose metabolism in Parkinson's disease with and without dementia. *Arch Neurol* 1992;**49**:1262–8.
29 **Eberling JL,** Richardson BC, Reed BR, *et al.* Cortical glucose metabolism in Parkinson's disease without dementia. *Neurobiol Aging* 1994;**15**:329–35.
30 **Bohnen NI,** Minoshima S, Giordani B, *et al.* Motor correlates of occipital glucose hypometabolism in Parkinson's disease without dementia. *Neurology* 1999;**52**:541–6.
31 **Hu MT,** Taylor-Robinson SD, Chaudhuri KR, *et al.* Cortical dysfunction in non-demented Parkinson's disease patients: a combined ^{31}P-MRS and ^{18}FDG-PET study. *Brain* 2000;**123**:340–52.
32 **Warrington EK,** James M, Kinsbourne M. Drawing disability in relation to laterality of cerebral lesion. *Brain* 1966;**89**:53–82.
33 **Benson DF,** Barton MI. Disturbances in constructional ability. *Cortex* 1970;**6**:19–46.
34 **Ikeda H,** Head GM, Ellis CJ. Electrophysiological signs of retinal dopamine deficiency in recently diagnosed Parkinson's disease and a follow up study. *Vision Res* 1994;**34**:2629–38.
35 **Jellinger KA.** Pathology of Parkinson's disease. Changes other than the nigrostriatal pathway. *Mol Chem Neuropathol* 1991;**14**:153–97.
36 **Hughes AJ,** Daniel SE, Blankson S, *et al.* A clinicopathologic study of 100 cases of Parkinson's disease. *Arch Neurol* 1993;**50**:140–8.
37 **Alexander GE,** Crutcher MD. Functional architecture of basal ganglia circuits: neural substrates of parallel processing. *Trends Neurosci* 1990;**13**:266–71.
38 **Parent A,** Hazrati LN. Functional anatomy of the basal ganglia. I. The cortico-basal ganglia-thalamo-cortical loop. *Brain Res Brain Res Rev* 1995;**20**:91–127.
39 **Denny-Brown D,** Yanagisawa N, Kirk E. The localization of hemispheric mechanism of visually directed reaching and grasping. In: Zülch KJ, Kreutzfeldt O, Galbraith GC, eds. *Cerebral localization.* Berlin: Springer, 1975:62–75.
40 **Denny-Brown D,** Yanagisawa N. The role of the basal ganglia in initiation of movement. In: Yahr M, ed. *The basal ganglia.* New York: Raven Press, 1976:115–49.
41 **Kemp JM,** Powell TP. The cortico-striate projection in the monkey. *Brain* 1970;**93**:525–46.

PAPER

Onset age and severity of motor impairment are associated with reduction of myocardial ^{123}I-MIBG uptake in Parkinson's disease

K Hamada, M Hirayama, H Watanabe, R Kobayashi, H Ito, T Ieda, Y Koike, G Sobue

J Neurol Neurosurg Psychiatry 2003;74:423–426

See end of article for authors' affiliations

Correspondence to: Dr G Sobue, Department of Neurology, Nagoya University Graduate School of Medicine, Nagoya 466–8550, Japan; sobueg@med.nagoya-u.ac.jp

Received 18 August 2002
In revised form 2 December 2002
Accepted 3 December 2002

Objectives: To elucidate the factors associated with severity of cardiac sympathetic nerve involvement in idiopathic Parkinson's disease (PD).
Methods: ^{123}I-metaiodobenzylguanidine uptake was examined in 88 patients with PD. The ratio of the uptake in the heart (*H*) to that in the mediastinum (M) (the *H/M* ratio) was calculated and correlated with age at onset, age at examination, and disease severity and duration. Twenty five healthy people were also examined as a control.
Results: There was a mild but significant negative correlation between *H/M* ratio and age at onset (early, $r = -0.33$, $p = 0.002$; delayed, $r = -0.34$, $p = 0.001$) and between Hoehn and Yahr (H-Y) stage (early, $r = -0.30$, $p = 0.006$; delayed, $r = -0.32$, $p = 0.003$). There was no significant correlation between disease duration and *H/M* ratio. When patients with PD were classified into four subgroups on the basis of age at onset (> 62 or < 62 years) and disease severity (H-Y > III or H-Y ≤ II), the median *H/M* ratio of the older and more severe group was significantly lower than that of the younger and less severe group ($p = 0.005$).
Conclusion: This study suggests that late onset, high severity PD is associated with myocardial sympathetic dysfunction.

^{123}I-metaiodobenzylguanidine (MIBG) is a physiological analogue of noradrenaline that traces the uptake and transport of noradrenaline in presynaptic sympathetic nerve terminals and subsequent vesicular storage.[1] Myocardial MIBG scintigraphy has been used to evaluate cardiac sympathetic nerve endings in both cardiac and various neurological diseases.[2–5] In idiopathic Parkinson's disease (PD), myocardial MIBG uptake is significantly reduced even without apparent autonomic failure, which enables early diagnosis of the illness.[6–17] Several studies involving small numbers of patients have suggested that duration and severity influence MIBG uptake in PD.[12 13 15] However, the factors proposed to be involved differ with the report. Furthermore, no previous study has investigated the effect of age at onset on MIBG cardiac uptake. In the present study, we examined the relations between myocardial MIBG uptake and age at onset, age at examination, disease severity, and disease duration in 88 patients with PD.

PATIENTS AND METHODS

From January 1997 to October 2001, myocardial MIBG scintigraphy was performed in 100 patients with PD according to the criteria of the United Kingdom Brain Bank.[18] None of the patients had familial or past histories of heart disease. All patients were examined by routine brain magnetic resonance imaging, and these results were incorporated into the diagnosis. Patients with Parkinson-plus syndrome or drug induced and postencephalitic parkinsonism were excluded. Twelve of the 100 patients with PD onset before reaching 45 years of age were excluded to differentiate autosomal recessive juvenile parkinsonism.[19] Thus, 88 patients with PD with the following characteristics were studied: 54 men and 34 women; mean (SD) age of onset 63.5 (9.6) years, range 45–85 years; mean age at examination 68.0 (9.0) years, range 49–87 years; mean disease duration 4.6 (3.6) years, range 1–12 years; and mean L-dopa intake 259 (174) mg. The Hoehn and Yahr (H-Y) scale was used to assess the severity of motor impairment: 10, 27, 40, 9, and 2 subjects were classified into stages I, II, III, IV, and V, respectively, when cardiac MIBG uptake was assessed. As a control group, 25 age matched people with no history of neurological or heart disease (13 men and 12 women, age at examination 66.6 (9.3) years) were enrolled in this study. We obtained informed consent from all subjects.

The 88 patients with PD were subgrouped based on the following cut off values: < 62 years old (younger), > 62 years old (older), H-Y ≤ II (mild), and H-Y > III (severe). Postural impairment is thought to result from a combined effect of the disease and aging processes, suggesting the widespread involvement of subcortical structures.[20] Consequently, patients with PD were classified into four groups: older/severe, older/mild, younger/severe, and younger/mild.

^{123}I-MIBG (111 mBq) was injected intravenously into each subject. The early image of cardiac uptake was taken 15 minutes later and the delayed image three or four hours later. Regions of interest were placed on the whole heart and mediastinum of the front image. The ratio of ^{123}I-MIBG uptake in regions of interest of the heart to that in the mediastinum (*H/M* ratio) was calculated. The *H/M* ratios from early and delayed images were evaluated in this study.

The Mann-Whitney U test was used for examining the intentional difference between two groups, the Kruskal-Wallis test was used for examining the intentional difference between three groups, and then Scheffé's F was used for post hoc testing. The relations between *H/M* ratio and age at onset, age at examination, and disease duration were analysed using Pearson's correlation coefficient. The relation between *H/M* ratio and H-Y scale was analysed using Spearman's correlation coefficient. Calculations were performed using the statistical

Abbreviations: H-Y, Hoehn and Yahr; MIBG, ^{123}I-metaiodobenzylguanidine; PD, Parkinson's disease

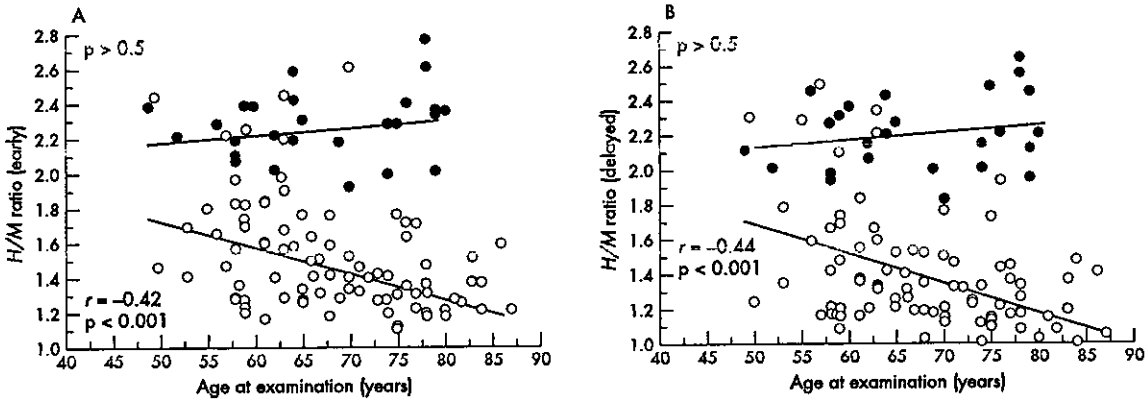

Figure 1 Age at examination had a significant negative correlation with heart to mediastinum (*H/M*) ratio in Parkinson's disease (PD) (PD patients: (A) early, $r = -0.42$, $p < 0.001$; (B) delayed $r = -0.44$, $p < 0.001$) but not in controls ($p > 0.5$). Open and closed circles represent individual patients with PD and control subjects, respectively.

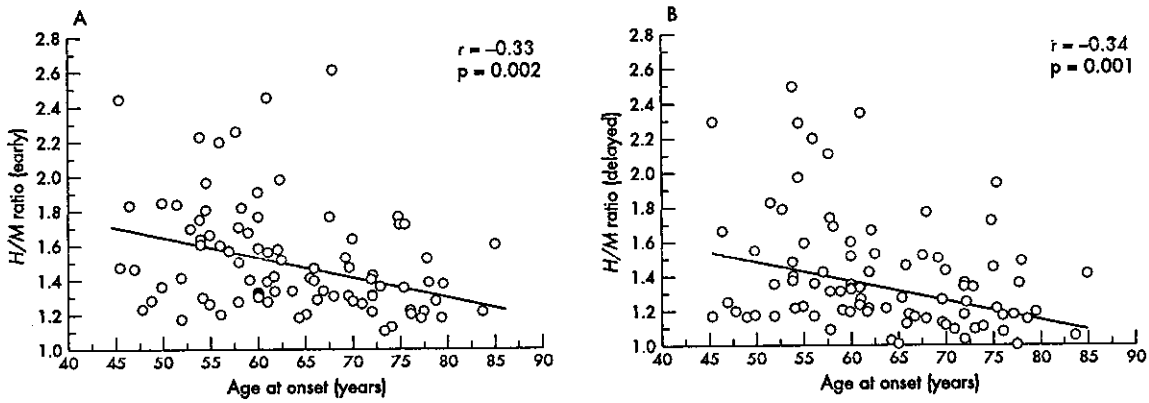

Figure 2 Age at onset had a slight but significant negative correlation with *H/M* ratio ((A) early, $r = -0.33$, $p = 0.002$; (B) delayed, $r = -0.34$, $p = 0.001$). Circles represent individual patients with PD.

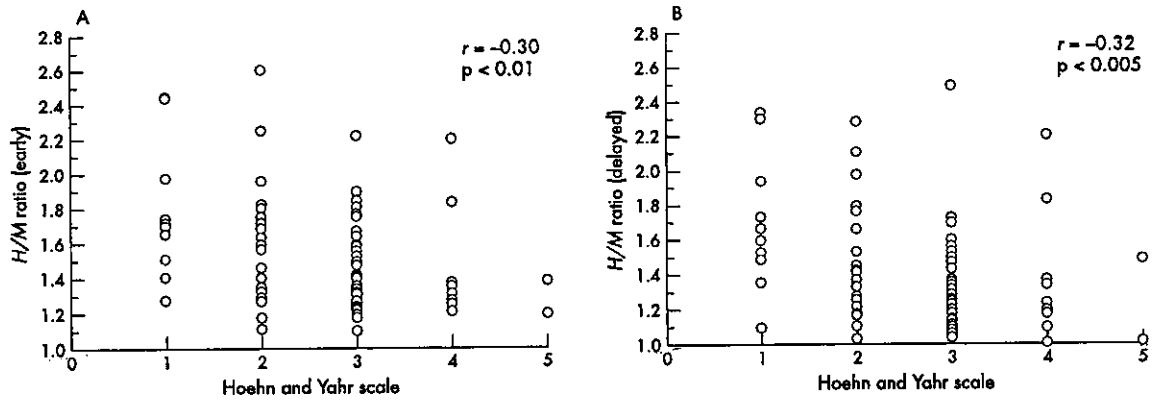

Figure 3 Hoehn and Yahr score had a slight but significant negative correlation with *H/M* ratio ((A) early, $r = -0.30$, $p < 0.01$; (B) delayed, $r = -0.32$, $p = 0.005$). Circles represent individual patients with PD.

software package StatView (Abacus Concepts, Berkeley, California, USA). The level of significance was defined at $p < 0.05$.

RESULTS

The *H/M* ratio of all patients with PD was significantly reduced compared with controls in both early (PD, 1.51 (0.32); control, 2.26 (0.19); $p < 0.0001$) and delayed images (PD, 1.39 (0.33); control, 2.19 (0.20); $p < 0.0001$).

The age at examination was correlated with *H/M* ratio in patients with PD (early, $r = -0.42$, $p < 0.001$; delayed, $r = -0.44$, $p < 0.001$; fig 1), while in control subjects this age dependent reduction was not observed ($p > 0.5$). The age at onset was mildly but significantly negatively correlated with *H/M* ratio in PD (early, $r = -0.33$, $p = 0.002$; delayed,

Table 1 Ratio of ^{123}I-metaiodobenzylguanidine uptake in the heart to that in the mediastinum in four subgroups of patients with Parkinson's disease and in healthy control subjects

	Early image		Delayed image	
Patient subgroup	Median	Range	Median	Range
Older/severe	1.30* **	1.10–1.76	1.17* **	0.90–1.76
Older/mild	1.40**	1.12–2.60	1.27**	1.03–1.93
Younger/severe	1.50**	1.16–2.22	1.31**	1.17–2.49
Younger/mild	1.63* **	1.27–2.45	1.42* **	1.09–2.34
Controls	2.26	1.92–2.77	2.19	1.93–2.55

*$p < 0.005$; **$p < 0.0001$ compared with controls.

$r = -0.34$, $p = 0.001$; fig 2), and the H-Y scale was mildly but significantly correlated with *H/M* ratio (early, $r = -0.30$, $p = 0.006$; delayed, $r = -0.32$, $p = 0.003$; fig 3). The disease duration was not, however, significantly correlated with *H/M* ratio (early, $r = -0.15$, $p = 0.16$; delayed, $r = -0.20$, $p = 0.07$).

When the patients with PD were classified into the four groups on the basis of age at onset and disease severity, the median *H/M* ratios of each of these groups were significantly reduced as compared with controls ($p < 0.001$; table 1). The *H/M* ratio was lowest in the older/severe group in both early and delayed images of the four groups. The difference in *H/M* ratio between the older/severe group and younger/mild group was significant ($p < 0.005$; table 1).

DISCUSSION

Age at onset and H-Y scale are negatively correlated with both early and delayed cardiac MIBG uptake as assessed by the *H/M* ratio. Furthermore, the combination of higher age at onset and advanced H-Y stage profoundly influenced the reduction of myocardial MIBG uptake in PD. On the other hand, the disease duration was not significantly correlated with either early or delayed MIBG uptake. Both the age at examination and age at onset were negatively correlated with the *H/M* ratio. The age at examination includes the age at onset and the disease duration, so age at onset has a greater influence on the *H/M* ratio.

Several possible explanations for the pathophysiology underlying low myocardial MIBG uptake in PD have been proposed. Whether myocardial MIBG uptake reflects sympathetic and systemic autonomic failure has not been verified, and the degree of *H/M* ratio reduction is not always associated with the presence of orthostatic hypotension conditions.[11 15 17] We, however, have previously shown that patients with PD with orthostatic hypotension display supersensitivity to noradrenaline[21] and severely decreased MIBG uptake of not only the myocardium but also the lower extremities.[7] Recently, Goldstein *et al* showed that patients with PD with orthostatic hypotension had much lower cardiac uptake of 6-[18F] fluorodopamine than those without the condition.[22] Furthermore, they showed that lower 6-[18F] fluorodopamine was seen not only in the myocardium but also in the thyroid and renal cortex in PD with orthostatic hypotension, although we did not measure MIBG uptake in these organs in this study. These findings suggest that the sympathetic nerves are involved more extensively in PD than previously believed. As a possible explanation for the discrepancy between the reduction of myocardial MIBG uptake and orthostatic hypotension in PD, myocardial sympathetic nerve dysfunction would precede generalised sympathetic denervation eliciting orthostatic hypotension. On the other hand, pathological studies have shown that Lewy bodies and Lewy neurites are commonly identified in the cardiac plexus in PD,[23] and tyrosine hydroxylase immunoreactive nerve fibres in the heart are greatly decreased in patients with orthostatic hypotension.[24] Taken together, the degree of decreased myocardial MIBG uptake is thought to reflect the severity of myocardial sympathetic involvement and to be correlated with systemic sympathetic nerve involvement in PD.

In this study, cardiac MIBG uptake was mildly but significantly correlated with age at onset in PD. In control subjects, however, there were no significant differences in cardiac MIBG uptake in terms of aging. This was in agreement with a previous study by Tsuchimochi *et al*,[25] who reported reduced MIBG uptake in the inferior regions in older patients but no significant decrease in the whole myocardium. They proposed that sympathetic neuronal function in the inferior region may be selectively disturbed with aging. However, we found that sympathetic neuronal function disturbance was more extensively associated with the age at onset of PD. Thus, the negative correlation between age at onset and whole myocardial MIBG uptake was specifically associated with PD, but not with normal aging. Patients with a later onset of PD may have increased motor disability associated with more extensive subcortical involvement.[26 27] Furthermore, the degree of dementia caused by the presence of Lewy bodies in cortical areas has been shown to be related to the age at onset.[28 29] These reports indicate that a later onset may be associated with widespread multisystem involvement in PD.

We found that cardiac MIBG uptake had a mild but significant negative correlation with H-Y stage. Furthermore, cardiac MIBG uptake was significantly reduced in patients with PD with an H-Y score > III compared with those with an H-Y score ≤ II. In general, autonomic dysfunction in PD becomes apparent as the disease progresses.[30] Our findings indicate that the cardiac sympathetic nerve may be involved in the advancing severity of motor impairment in PD.

Patients with PD often have combinations of motor impairment, cognitive disorder, and autonomic failure during the course of the illness. However, the temporal progression of these three symptoms is heterogeneous among patients. Various factors have been proposed to influence the progression of PD. The present results suggest that patients with PD who have a combination of later onset and more severe clinical stage have increasing cardiac sympathetic nerve impairment in PD. Levy *et al*[31] reported that the increase in risk of dementia in PD was associated primarily with the combined effects of age and the severity of extrapyramidal signs.[31] Our findings are similar to those of Levy *et al* and suggest that later onset PD with high severity comes with an increased risk of early evolution not only to motor and cognitive system involvement but also to myocardial sympathetic involvement.

PD varies between patients in several respects, including age at onset and the rates of progression of both the severity of motor impairment and the involvement of multiple systems. Understanding the progression pattern of PD would provide novel targets for curative treatments on the basis of molecular and environmental studies. However, further prospective studies are needed to determine why age at onset and the severity of motor impairment are associated with reduced myocardial MIBG uptake in PD.

Authors' affiliations
K Hamada, M Hirayama, H Watanabe, R Kobayashi, H Ito, G Sobue, Department of Neurology, Nagoya University Graduate School of Medicine, Nagoya, Japan
T Ieda, Department of Neurology, Yokkaichi Municipal Hospital, Yokkaichi, Japan
Y Koike, Department of Medical Technology, Nagoya University School of Health Sciences, Nagoya, Japan

REFERENCES

1 **Wieland DM,** Wu JL, Brown LE, *et al.* Radiochemistry and radiopharmaceurticals: radiolabeled adrenergic neuron-blocking agents: adrenomedullary imaging with I-131 iodobenzylguanidine. *J Nucl Med* 1980;**21**:349–53.
2 **Stanton MS,** Tuli MM, Radike NL, *et al.* Regional sympathetic denervation after myocardial infarction in humans detected noninvasively using I-123 metaiodobenzylguanidine. *J Am Coll Cardiol* 1989;**14**:1519–26.
3 **Mantyasaari M,** Kuikka J, Mustonen J, *et al.* Noninvasive detection of cardiac sympathetic nervous dysfunction in diabetic patients using 123I-metaiodobenzylguanidine. *Diabetes* 1992;**41**:1069–75.
4 **Watanabe H,** Ieda T, Katayama T, *et al.* Cardiac ^{123}I-meta-iodobenzylguanidine (MIBG) uptake in dementia with Lewy bodies: comparison with Alzheimer's disease. *J Neurol Neurosurg Psychiatry* 2001;**70**:781–3.
5 **Watanabe H,** Misu K, Hirayama M, *et al.* Low cardiac ^{123}I-MIBG uptake in late-onset familial amyloid polyneuropathy type I (TTR Met30). *J Neurol* 2001;**248**:627–9.
6 **Hakusui S,** Yasuda T, Yanagi T, *et al.* A radiological analysis of heart sympathetic functions with meta-[123I]iodobenzylguanidine in neurological patients with autonomic failure. *J Auton Nerv Syst* 1994;**49**:81–4.
7 **Hirayama M,** Hakusui S, Koike Y, *et al.* A scintigraphical qualitative analysis of peripheral vascular sympathetic function with meta-[123I]iodobenzylguanidine in neurological patients with autonomic failure. *J Auton Nerv Syst* 1995;**53**:230–4.
8 **Yoshita M,** Hayashi M, Hirai S. Decreased myocardial accumulation of 123I-meta-iodobenzyl guanidine in Parkinson's disease. *Nucl Med Commun* 1998;**19**:137–42.
9 **Yoshita M.** Differentiation of idiopathic Parkinson's disease from striatonigral degeneration and progressive supranuclear palsy using iodine-123 meta-iodobenzylguanidine myocardial scintigraphy. *J Neurol Sci* 1998;**155**:60–7.
10 **Iwasa K,** Nakajima K, Yoshikawa H, *et al.* Decreased myocardial 123I-MIBG uptake in Parkinson's disease. *Acta Neurol Scand* 1998;**97**:303–6.
11 **Braune S,** Reinhardt M, Bathmann J, *et al.* Impaired cardiac uptake of meta-[123I]iodobenzylguanidine in Parkinson's disease with autonomic failure. *Acta Neurol Scand* 1998;**97**:307–14.
12 **Satoh A,** Serita T, Seta M, *et al.* Loss of 123I-MIBG uptake by the heart in Parkinson's disease: assessment of cardiac sympathetic denervation and diagnostic value. *J Nucl Med* 1999;**40**:371–5.
13 **Orimo S,** Ozawa E, Nakade S, *et al.* ^{123}I-metaiodobenzylguanidine myocardial scintigraphy in Parkinson's disease. *J Neurol Neurosurg Psychiatry* 1999;**67**:189–94.
14 **Braune S,** Reinhardt M, Schnitzer R, *et al.* Cardiac uptake of [123I]MIBG separates Parkinson's disease from multiple system atrophy. *Neurology* 1999;**53**:1020–5.
15 **Takatsu H,** Nishida H, Matsuo H, *et al.* Cardiac sympathetic denervation from the early stage of Parkinson's disease: clinical and experimental studies with radiolabeled MIBG. *J Nucl Med* 2000;**41**:71–7.
16 **Druschky A,** Hilz MJ, Platsch G, *et al.* Differentiation of Parkinson's disease and multiple system atrophy in early disease stages by means of I-123-MIBG-SPECT. *J Neurol Sci* 2000;**175**:3–12.
17 **Taki J,** Nakajima K, Hwang EH, *et al.* Peripheral sympathetic dysfunction in patients with Parkinson's disease without autonomic failure is heart selective and disease specific. *Eur J Nucl Med* 2000;**27**:566–73.
18 **Daniel SE,** Less AJ. Parkinson's Disease Society Brain Bank, London: overview and research. *J Neural Transm Suppl* 1993;**39**:165–72.
19 **Oliveri RL,** Zappia M, Annesi G, *et al.* The parkin gene is not involved in late-onset Parkinson's disease. *Neurology* 2001;**57**:359–62.
20 **Levy G,** Tang MX, Cote LJ, *et al.* Motor impairment in PD: relationship to incident dementia and age. *Neurology* 2000;**55**:539–44.
21 **Niimi Y,** Ieda T, Hirayama M, *et al.* Clinical and physiological characteristics of autonomic failure with Parkinson's disease. *Clin Auton Res* 1999;**9**:139–44.
22 **Goldstein DS,** Holmes CS, Dendi R, *et al.* Orthostatic hypotension from sympathetic denervation in Parkinson's disease. *Neurology* 2002;**58**:1247–55.
23 **Iwanaga K,** Wakabayashi K, Yoshimoto M, *et al.* Lewy body-type degeneration in cardiac plexus in Parkinson's and incidental Lewy body diseases. *Neurology* 1999;**52**:1269–71.
24 **Orimo S,** Ozawa E, Oka T, *et al.* Different histopathology accounting for a decrease in myocardial MIBG uptake in PD and MSA. *Neurology* 2001;**57**:1140–1.
25 **Tsuchimochi S,** Tamaki N, Tadamura E, *et al.* Age and gender differences in normal myocardial adrenergic neuronal function evaluated by iodine-123-MIBG imaging. *J Nucl Med* 1995;**36**:969–74.
26 **Granerus AK,** Carlsson A, Svanborg A, *et al.* The aging neuron influence on symptomatology and therapeutic response in Parkinson's syndrome. *Adv Neurol* 1979;**24**:327–34.
27 **Blin J,** Dubois B, Bonnet AM, *et al.* Does aging aggravate parkinsonian disability? *J Neurol Neurosurg Psychiatry* 1991;**54**:780–2.
28 **Hurtig HI,** Trojanowski JQ, Galvin J, *et al.* Alpha-synuclein-cortical Lewy bodies correlate with dementia in Parkinson's disease. *Neurology* 2000;**54**:1916–21.
29 **Apaydin H,** Ahlskog JE, Parisi JE, *et al.* Parkinson's disease neuropathology. Later-developing dementia and loss of the levodopa response. *Arch Neurol* 2002;**59**:102–12.
30 **Koike Y,** Takahashi A. Autonomic dysfunction in Parkinson's disease. *Eur Neurol* 1997;**38**(suppl 2):8–12.
31 **Levy G,** Schupf N, Tang MX, *et al.* Combined effect of age an severity on the risk of dementia in Parkinson's disease. *Ann Neurol* 2002;**51**:722–9.

Heat Shock Protein 70 Chaperone Overexpression Ameliorates Phenotypes of the Spinal and Bulbar Muscular Atrophy Transgenic Mouse Model by Reducing Nuclear-Localized Mutant Androgen Receptor Protein

Hiroaki Adachi,[1] Masahisa Katsuno,[1] Makoto Minamiyama,[1] Chen Sang,[1] Gerassimos Pagoulatos,[2] Charalampos Angelidis,[2] Moriaki Kusakabe,[3] Atsushi Yoshiki,[4] Yasushi Kobayashi,[1] Manabu Doyu,[1] and Gen Sobue[1]

[1]Department of Neurology, Nagoya University Graduate School of Medicine, 65 Tsurumai-cho Showa-ku, Nagoya 466-8550, Japan, [2]Department of General Biology, University of Ioannina, School of Medicine, Ioannina GR-45110, Greece, [3]ANB Tsukuba Institute, ALOKA Company, Ltd., 1103 Fukaya, Kasumigaura, Niihari, Ibaraki 300-0134, Japan, and [4]Experimental Animal Division, Department of Biological Systems, BioResource Center, The Institute of Physical and Chemical Research (RIKEN) Tsukuba Institute 3-1-1 Koyadai, Tsukuba, Ibaraki 305-0074, Japan

Spinal and bulbar muscular atrophy (SBMA) is an inherited motor neuron disease caused by the expansion of the polyglutamine (polyQ) tract within the androgen receptor (AR). The nuclear inclusions consisting of the mutant AR protein are characteristic and combine with many components of ubiquitin–proteasome and molecular chaperone pathways, raising the possibility that misfolding and altered degradation of mutant AR may be involved in the pathogenesis. We have reported that the overexpression of heat shock protein (HSP) chaperones reduces mutant AR aggregation and cell death in a neuronal cell model (Kobayashi et al., 2000). To determine whether increasing the expression level of chaperone improves the phenotype in a mouse model, we cross-bred SBMA transgenic mice with mice overexpressing the inducible form of human HSP70. We demonstrated that high expression of HSP70 markedly ameliorated the motor function of the SBMA model mice. In double-transgenic mice, the nuclear-localized mutant AR protein, particularly that of the large complex form, was significantly reduced. Monomeric mutant AR was also reduced in amount by HSP70 overexpression, suggesting the enhanced degradation of mutant AR. These findings suggest that HSP70 overexpression ameliorates SBMA phenotypes in mice by reducing nuclear-localized mutant AR, probably caused by enhanced mutant AR degradation. Our study may provide the basis for the development of an HSP70-related therapy for SBMA and other polyQ diseases.

Key words: **HSP70; chaperone; polyglutamine; SBMA; transgenic mice; protein degradation**

Introduction

Polyglutamine (polyQ) diseases are inherited neurodegenerative disorders caused by the expansion of a trinucleotide CAG repeat in the causative genes (Zoghbi and Orr, 2000). To date, nine polyQ diseases have been identified (Ross, 2002). Spinal and bulbar muscular atrophy (SBMA) is a polyQ disease, characterized by proximal muscle atrophy, weakness, contraction fasciculations, and bulbar involvement (Kennedy et al., 1968; Sobue et al., 1989; Takahashi, 2001). In SBMA, a polymorphic CAG repeat with 14–32 CAGs expands to 40–62 CAGs in the first exon of the androgen receptor (*AR*) gene (Tanaka et al., 1996) and has somatic mosaicism (Tanaka et al., 1999). There is an inverse correlation between the CAG repeat size and the age at onset or the disease severity in SBMA (Doyu et al., 1992; Igarashi et al., 1992; La Spada et al., 1992). In SBMA, nuclear inclusions (NIs) containing mutant AR have been observed in the brainstem motor nuclei, spinal motor neurons, and some visceral organs (Li et al., 1998a,b). Such neuronal inclusions are common pathological features in polyQ diseases and are also colocalized with many components of ubiquitin–proteasome and molecular chaperones (Chai et al., 1999; Huynh et al., 2000; Adachi et al., 2001; Zander et al., 2001; Schmidt et al., 2002), raising the possibility that misfolding and altered degradation of the mutant protein may be involved in the pathogenesis of SBMA as well as other polyQ diseases (Stenoien et al., 1999; Waelter et al., 2001). Furthermore, these chaperones and proteasomes would facilitate refolding or proteolysis of the mutant protein and may play a role in protecting neuronal cells against the toxic properties of the expanded polyQ (Cummings et al., 1998; Kobayashi et al., 2000). We have shown recently that overexpression of heat shock proteins (HSPs) decreases the aggregate formation of truncated AR with the expanded polyQ and markedly prevents cell death in the neuronal cell model of SBMA (Kobayashi et al., 2000; Kobayashi and Sobue, 2001). HSP70 overexpression has been reported to enhance the solubility and degradation of mutant AR (Bailey et al., 2002). HSPs have also been shown to suppress aggregate formation and cellular toxicity in a wide range of polyQ disease models (Cummings et al., 1998; Warrick et al., 1999; Carmichael et al., 2000). Recently, overexpression of the inducible form of rat

Received Nov. 5, 2002; revised Dec. 31, 2002; accepted Dec. 31, 2002.

This work was supported by a Center of Excellence grant from the Ministry of Education, Culture, Sports, Science, and Technology of Japan and by grants from the Ministry of Health, Labor, and Welfare of Japan. We thank Sugiko Yokoi for her technical assistance.

Correspondence should be addressed to Dr. Gen Sobue, Department of Neurology, Nagoya University Graduate School of Medicine, 65 Tsurumai-cho Showa-ku, Nagoya, 466-8550, Japan. E-mail: sobueg@med.nagoya-u.ac.jp.

 0270-6474/03/232203-09$15.00/0